Monitoring Hydrologic Controls on Biogeochemical Process Variability in Green Infrastructure Soils

Laine Pulvermacher
Marquette University

MONITORING HYDROLOGIC CONTROLS ON BIOGEOCHEMICAL PROCESS VARIABILITY IN GREEN INFRASTRUCTURE SOILS

by

Laine Pulvermacher

A Thesis submitted to the Faculty of the Graduate School,
Marquette University,
in Partial Fulfillment of the Requirements for
the Degree of Master of Science

Milwaukee, Wisconsin

May 2020

ABSTRACT

MONITORING HYDROLOGIC CONTROLS ON BIOGEOCHEMICAL PROCESS VARIABILITY IN GREEN INFRASTRUCTURE SOILS

Laine Pulvermacher

Marquette University, 2020

The premise of this research was to monitor biogeochemical responses to soil moisture and soil temperature within green stormwater infrastructure soils. Adopting best management practices like green infrastructure in urban areas has the potential to remove incoming nutrients from stormwater runoff through biogeochemical processes, like plant and microbial metabolism. Biogeochemical activity has been suggested to be highly variable, so this research proposed to monitor that variability by tracking the stoichiometry of soil respiration. Additionally, an advection-diffusion-reaction model was used to disaggregate physical and biogeochemical controls on the observed soil respiration.

The field data was collected to investigate the biogeochemical processes, their response to soil conditions, and their spatial and temporal variability. Field results showed soil respiration increased with soil moisture at all sites except a wetland lowland plot. The model simulations from the advection-diffusion-reaction model suggested that the soil gas response to soil moisture was driven by biogeochemical process rates rather than the physical processes of gas transport. Soil temperature was related to soil respiration, but the relationship depended on the season and green infrastructure site.

The monitored gas concentrations in the green infrastructure soils suggested the carbon dioxide was lower than what is needed for soil respiration to be the main driver of the gas ratios. Instead, abiotic processes like carbon dioxide dissolution or biotic processes like methanogenesis metabolism may be decreasing the carbon dioxide concentrations. Additionally, the field soils may be well aerated causing the oxygen concentrations to be higher than anticipated soil concentrations if soil respiration was the main biogeochemical process driving the gas concentrations. There is little known about the biogeochemistry of green infrastructure soils, and more studies are needed for improved understanding of these engineered systems, including better identifying the biogeochemical processes, modeling the systems, and long-term monitoring.

ACKNOWLEDGEMENTS

Laine Pulvermacher

I would like to express my sincere appreciation to my major advisor, Dr. Anthony Parolari, for his knowledge and guidance throughout my research. I also extend thanks to my other committee members, Dr. Brooke Mayer and Dr. Walter McDonald for their valuable support and assistance in reviewing my thesis. Thanks to the entire Water Resource Lab and Water Quality Center at Marquette University for their continued support throughout my research. I would like to specifically thank Sazzad Sharior, Isabelle Horvath, Duyen Lam, Gerardo Ornelas Rodriguez, Joseph Sizemore, Tom Silman, and David Newman for their assistance and guidance in the green infrastructure data collection and set ups used in my research. Your help was invaluable toward the success of my research. Also, I would like to thank the Marquette University Department Fellowship for funding and support of this research. Thanks also to the faculty at the Marquette University Department of Civil and Environmental Engineering along with the faculty at the Marquette University's Discovery Learning lab for their valuable support and assistance throughout my research. Finally, I would like to thank my husband, Matt Pulvermacher, and to my family and friends for their continued love and support.

TABLE OF CONTENTS

1. INTRODUCTION

This study examines the biogeochemical process response to hydrologic conditions in green stormwater infrastructure (GSI). Together with soil moisture and temperature measurements, the apparent respiratory quotient (ARQ) was monitored with measured oxygen and carbon dioxide concentrations in the soil. An advection-diffusion-reaction model was then used to identify if physical or biogeochemical processes control the ARQ.

1.1 Motivation for Work

Nutrients, like nitrogen (N) and phosphorus (P), are compounding in environments due to excessive use, synthetic fertilizer creation, burning of fossil fuels, and atmospheric deposition. Accordingly, nutrient pollution is an increasing threat to water resources. Water issues like eutrophication and hypoxia in natural water sources have been linked to the presence of both N and P (Conley et al., 2009; Smith et al., 2015; Smith et al., 1999). Nationally, the presence of nutrients contributes to the biological impairment of 46% of the rivers and streams and hypereutrophic conditions in 21% of the lakes (EPA, 2017). Locally, total P polluted 76% of impaired waterbodies in Wisconsin in 2018 (WDNR, 2018). Additionally, excess nutrients can be a health concern; for example, high nitrate (NO_3) levels are directly linked to blue baby syndrome (methemoglobinemia) (Knobeloch et al., 2000). Although P is not associated with direct human health concerns, it promotes growth of algae that release toxins, which can be detrimental to human health (EPA, 2019). The ability to track and manage the N cycle is

one of the top fourteen greatest engineering challenges, according to the National Academy of Engineering (NAE, 2012).

Urban areas are of concern for nutrient pollution in waters due to the high percentage of impervious surfaces that allow for the extra nutrients to wash off into surface waters. For example, in the Baltimore Ecosystem Study, urban and suburban watersheds were shown to have nearly eight times higher N loss than a completely forested watershed (Groffman et al., 2004). In response, urban best management practices, such as GSI, are encouraged for capturing pollutants (i.e., N and P) before entering surface waters to improve these water quality issues (Field et al., 2004). Stormwater caught in terrestrial environments can promote nutrient removal processes like filtration and biological conversion of nutrients (Davis et al., 2010). However, GSI nutrient retention and removal have proven to be ambiguous with GSI acting as either a nutrient sink or source (Bratieres et al., 2008; Daly et al., 2012; Hatt et al., 2009; Hunt et al., 2006; Li & Davis, 2014).

Studying processes that impact nutrient uptake may unlock the uncertainty around the ability of GSI to remove or store nutrients. GSI can remove incoming nutrients from water by biogeochemical processes or by physical processes like filtration (Davis, 2007). Biogeochemical process activity is linked to the availability of N and P (Schlesinger & Bernhardt, 2013) and was shown to change in urbanized environments due to climatic changes (Bettez & Groffman, 2012; Groffman & Crawford, 2003). High variability of biogeochemical activity in GSI systems can lead to dissolved chemical forms of N and P leaving GSI after storm events (Li & Davis, 2014; Liu & Davis, 2014). Meanwhile, studies have shown that particulate N and P forms are collected in GSI after a storm event

through physical processes (Li & Davis, 2014; Liu & Davis, 2014) until eventually the GSI no longer can filter the nutrients and begins to release particulate nutrients (Buffam & Mitchell, 2015; Davis, 2005). Soil has a limited ability to filter particulate-bound nutrients, therefore, GSI design efforts must also focus on promoting biogeochemical activity to transform and remove nutrients from stormwater (Davis, 2005). This study monitored gas concentrations associated with biogeochemical processes, volumetric water content (VWC), and soil temperature at a high frequency to test the variability of biogeochemistry linked to soil conditions in GSI.

1.2 Objectives

This work aimed to unravel unknowns about the variability of biogeochemistry in engineered GSI systems. The goal of this research was to understand how biogeochemical processes respond to variable hydrologic and climatic conditions at a high frequency to distinguish between biotic and abiotic, as well as aerobic or anaerobic processes. A parameter known as the apparent respiratory quotient (ARQ) was used to represent the variability of biogeochemical processes. The ARQ is the ratio of the CO_2 efflux to the O_2 influx and is representative of the biogeochemical reactions occurring in soils. The study included two objectives. The first objective was to determine if soil moisture and/or temperature can predict the variability of the ARQ. It was hypothesized that soil biogeochemical activity is driven by the soil hydrologic conditions at high frequencies. The second objective was to utilize an advection-diffusion-reaction model to test if physical or biogeochemical processes drive the temporal variability in the ARQ. It

was hypothesized that the variability of gas concentrations in response to hydrological conditions was more related to biogeochemical processes than physical processes.

2. LITERATURE REVIEW

2.1 General Goals of GSIs

Stormwater runoff is recognized as a major pollutant source as the runoff picks up nutrients from impervious surfaces in urban areas and carries them to bodies of water (EPA, 2017). In urban areas, impervious surfaces prevent rainfall from infiltrating into soils. High imperviousness of urban surfaces and flooding when precipitation falls in an urban area creates the "urban stream syndrome" (Paul & Meyer, 2001; Walsh et al., 2005). The urban stream syndrome, described as stream degradation due to urban runoff, is of concern not only for its impacts on watershed hydrographs but also on water quality. Altering as low as 8-12% of the land imperviousness can negatively impact water quality (Wang et al., 2001).

GSI addresses stormwater runoff concerns by decreasing runoff volume, peak flow, and nutrient load by recreating natural hydrological and biogeochemical functions (Nylen & Kiparsky, 2015; EPA, 2010). Empirical and modeling studies of GSI have demonstrated promising performance for infiltration and reducing peak flow (Avellandeda et al., 2017; Jarden et al., 2016; Yang & Li, 2013). But, GSI catchment regulations vary by location. For example, San Jose requires control of 10% of a 50-year peak flow whereas Chicago requires control of 0.5-inch runoff from all impervious surfaces (EPA, 2010). Due to these differences in stormwater regulations, GSI size and operational protocols can be different and therefore result in different reductions in peak flows and nutrient loads. If GSI can decrease nutrient loads to surface waters, then many

water quality issues caused by urban stormwater runoff such as eutrophication may be lessened. Although the goals of GSI align well with urban area needs, the processes and biogeochemical interactions in soils of these engineered systems have not been addressed (Bratieres et al., 2008). Biogeochemical processes within the soil control how nutrients, like N and P, are removed by plant or microbial metabolism (Burgin et al., 2011), P sequestration by metals (Okochi & McMartin, 2011), and N reduction-oxidation processes (Gao et al., 2010).

2.2 GSI Performance in Nutrient Treatment

Studies report GSI performance to capture and treat influent stormwater to be variable (Bettez & Groffman, 2012; Collins et al., 2010; Dietz & Clausen, 2005; Li & Davis, 2014; Newcomer Johnson et al., 2014; Norton et al., 2017; Pataki et al., 2011; Payne et al., 2014). GSI nutrient removal depends on plant and microbial uptake, redox respiration processes, metal sorption, and adsorption to soil, with efficiencies varying between studies (Collins et al., 2010). Some GSI studies have shown positive N retention, e.g., retaining 150 times more total dissolved N (g/day) than for a system directly discharging to a stream (Newcomer Johnson et al., 2014). However, some studies have shown negative results, e.g., a bioretention study showed the system had more NO_3 and dissolved organic nitrogen (DON) in the effluent than in the influent (Li & Davis, 2014). The inadequate N removal of the system could be due to high organic matter used in the system and aerobic transformation of the organic N and ammonia to NO_3, which is highly mobile, between intermittent storms (Li & Davis, 2014). Overall, the ability to capture nutrients in GSI varies from nutrient load reductions of 10 to 75%, and the GSI can even

be a source of nutrients (Bratieres et al., 2008; Hunt et al., 2006). GSI design and materials may explain this variable performance.

The bioretention study by Li and Davis (2014) found that total dissolved N, as well as NO_3, was higher in the effluent leaving the bioretention system than entering the system, suggesting low biological activity. NO_3 and ammonium (NH_4) are N species that are readily taken up by organisms for growth (Marschner, 2012), so when NO_3 leaves the systems, this suggests organisms are not actively taking it up or the NO_3 supply exceeds plant and microbial demand. Likewise, a GSI study database reported median removal efficiency (5 studies) of soluble P (ortho-phosphorus and dissolved P) as -9% in bioretention systems (CWP, 2007). Soluble P is plant available but is also likely to leach or dissolve in runoff (Berg et al., 2018). The bioretention system study by Liu and Davis (2014), that looked at the fate of P species when 5% of soils are amended with aluminum or iron-based water treatment residuals, found that approximately 40% of both soluble reactive P and dissolved organic P was released through the underdrain. However, the particulate phosphorus (PP) decreased after entering the bioretention system, where the PP in the effluent was less than 0.1 mg/L for 96% of the time, suggesting the soil is physically filtering the nutrients (Liu & Davis, 2014). These studies draw attention to the activity of biogeochemical processes in these systems, suggesting the GSI soils relied more on physical processes than biogeochemical processes for pollutant removal.

There are rising concerns that the GSI design and materials, including plants and soil media, can impact the effectiveness of the infrastructure to remove nutrients. Compost has been noted to increase the N and P runoff in the effluent from GSI (Chahal et al., 2016; Hurley et al., 2017; Li & Davis, 2014). Utilizing woodchips can create

biofilms that increase denitrification rates (Lopez-Ponnada et al., 2017) and can be used as a carbon source for denitrifiers in urban soils (Kim et al., 2003). Substrates used in green roofs are high in nutrients, creating a source of N and P runoff for as long as decades in the case of P (Buffam & Mitchell, 2015). Finding the optimal design for GSI has been no easy feat and one favorable GSI design may not apply to other GSI types. For example, bioretention systems that are connected and flow into one another through an underdrain demonstrated high N removal (Wang et al., 2017). However, for rain garden designs that are connected to an underdrain that discharges to a stormwater system achieved a low pollutant retention (Bannerman & Considine, 2003; Dietz & Clausen, 2005). Studies conducted using soil columns found that plant species are an influential component in the ability of biofilters to remove N (Bratieres et al., 2008; Wang et al., 2017). Managing the vegetation, such as removing the dead or clipped vegetation when dormant, can result in reductions of P and N in GSI soils (Davis et al., 2006). Hatt et al. (2007) found that a media depth of at least 0.5 meters, as well as the inclusion of a gravel filter layer on top, decreased sediment and metals before clogging, but did not consistently decrease total P and total N. Therefore, soil type, soil depth, plant species, and management all contribute to the ability of GSI to remove pollutants.

In addition to GSI materials and design, the performance variability of GSI was suggested by several studies to be related to soil hydrology and climate. A study comparing dry to wet stormwater detention basins found that the wet detention basins had significantly higher denitrification potentials than the dry detention basins (McPhillips & Walter, 2015). Additionally, high denitrification rates and N retention were found to be related to saturated conditions in locations like bioretention swales and roadside ditches

(McPhillips et al., 2016; Norton et al., 2017). Soil moisture content explained 56% of denitrification potential in enhanced tree pits, infiltration swales, vegetation swales, and urban forest (Deeb et al., 2018). It was found that including an internal water storage zone in a bioretention system showed higher NO_3 removal rates than a bioretention system without a water storage zone (Hunt et al., 2006). A study on the ability of a biofilter system to treat nutrients in cold temperatures found that N species (NO_x) were not effectively treated at 8 °C and 2 °C (Blecken et al., 2007). The biological influence on removing N was suggested to be limited at those temperatures, thus increasing dissolved N and NO_x (Blecken et al., 2007).

2.3 GSI Nutrient Cycling and Pollutant Removal Efficiency Dependence on Biogeochemistry

Monitoring biogeochemical activity can assist in understanding the nutrient cycle by determining the nutrient fates (Lin et al., 2014). Biogeochemical activity can fluctuate at a high frequency in response to environmental conditions such as oxygen availability (Pett-Ridge et al., 2006; Rode et al., 2016). However, the biogeochemical activity of urban GSI have yet to be monitored at a high frequency. The biogeochemistry is relatively unknown in these engineered systems in comparison to agricultural or non-engineered systems (Pataki et al., 2011).

Due to human impacts, the biogeochemistry within the urban soils is different from the well-studied agricultural and natural ecosystems (Kaye et al., 2006; Pouyat et al., 2010). Synthetic fertilizers applied to urban soil increase the mass of nutrients in the system, thus creating an imbalance and unknown fate of the excess nutrients (Carey et al., 2013). Urban areas also contributed to sources of N by employing fossil fuel combustion

in addition to fertilizer application (Zhu et al., 2005). This addition of N can alter biogeochemistry in urban soils. For example, increased denitrification rates in urban soils were found to be among the highest rates recorded (Zhu et al., 2005). In urban watersheds, major contributors to the P cycle are pet waste and atmospheric deposition (Hobbie et al., 2017).

Chemical reactions assist in processing incoming nutrients and such reactions are influenced by the pH of the environment. For example, the relative fractions of NO_3 and NH_4 depend on the soil pH, which controls nitrification (Dancer et al., 1973; Sahrawat, 1982; Strauss et al., 2002). Additionally, pH is an influencer of soil microbial communities, as reported in a bacterial rDNA study that found that pH explained 70% and 58% of the microbial diversity and richness, respectively (Fierer & Jackson, 2006). One study suggested that soil with a neutral pH has a lower risk of nutrient contamination than soil with a low pH because their reported nitrification potentials (μg-N/g dry soil/day) decreased with pH (Deeb et al., 2018). Due to pH influence on nutrients and biological activity, pH effects biogeochemistry (Soetaert et al., 2007).

Physical aspects of soil also control the soil biogeochemistry. Soil type is a physical driver of biogeochemistry and the presence of substances like carbon, N, and P (Jiao et al., 2016). The soil type influences the water capacity of the soil, the minerals present and by extension pH and elements, as well as biological activity (i.e., compacted clay restricts root extension growth). Many GSI manuals suggest using soil types that promote high infiltration, such as coarse sand (e.g., DNR, 2014; Livingston et al., 2019).

Soil biogeochemistry is highly dynamic and responds to hydro-climatic variability in temperature and soil moisture. However, direct measurements of biogeochemical

responses to hydro-climatic fluctuations have not been made in urban soils to better understand the biogeochemistry within the engineered systems. Variable soil moisture and temperature have been shown to influence biogeochemical processes such as organic matter decomposition (Sierra et al., 2017), geological and chemical weathering (Maher & Chamberlain, 2014; White & Blum, 1995), methanogenesis (Moore & Dalva, 1993), denitrification (Fenchel et al., 2012), and soil respiration (Hicks Pries et al., 2019). Although researchers have studied relationships between biogeochemistry and hydro-climatic conditions, soil biogeochemistry responses to variable soil moisture and temperature have not been studied in engineered urban soils. These systems are needed to treat nutrients in stormwater runoff; therefore, studying soil processes in them will help bridge a gap in understanding of GSI nutrient removal performance.

2.4 Monitoring Biological Respiration

Abiotic reactions like weathering and oxidation, have been monitored in soils for decades (Lasaga, 1984; Patrick & Jugsujinda, 1992; White & Blum, 1995). Recent research has investigated biological activity and monitoring due to its role in elemental cycling, primarily carbon (Amundson et al., 2007; Angert et al., 2015; Calmels et al., 2014; Ferraz de Almeida et al., 2018; Sierra et al., 2017). One way to monitor biological activity at a high frequency is to measure respiration stoichiometry with O_2 and CO_2 concentrations.

Monitoring biological activity at a high frequency is essential as others have reported variability due to seasonal or event-based changes in hydro-climatic conditions (Hicks Pries et al., 2019; Lloyd & Taylor, 1994; Olshansky et al., 2019; Sierra et al.,

2017). Diurnal temperature changes have been correlated to hysteresis responses from respiration (Zhang et al., 2015). Examples of the hysteresis response include reports of high soil respiration occurring in the mid-morning in response to diurnal temperature fluctuations, but higher soil moisture contents slowing the diffusion rate, which causes a lag between CO_2 production and diffusion (Riveros-Iregui et al., 2007; Zhang et al., 2018). Seasonal changes in soil moisture and temperature may be attributed to differences in respiration rates (Hicks Pries et al., 2019; Hodges et al., 2019; Law et al., 1999). Low soil moisture can cause microbial and root metabolism to decrease (Li et al., 2015), while higher moisture, caused by precipitation events, may increase respiration rates (Sierra et al., 2017). Saturated soil can decrease O_2 availability due to reduced gas diffusivity that prevents reaeration of the soil from the atmosphere promoting anaerobic metabolism (Liptzin et al., 2011; Silver et al., 1999). Soil moisture is variable, however, resulting in potentially highly variable biological activity. Fine-scale temporal variability of respiration and the response to soil moisture have yet to be analyzed in urban soils.

Customarily, soil CO_2 measurements have been used as a proxy for soil respiration, using either a gradient or chamber method (Davidson et al., 2002; Fang & Moncrieff, 1998). However, because soil CO_2 participates in a range of processes, it is not a reliable representation of solely soil respiration. With geochemical processes, CO_2 takes part in both the silicate and carbonate cycles. A portion of CO_2 formed in the soil will leach into the groundwater at a rate of around 0.2 gigatons per year (Kessler & Harvey, 2001). Additionally, CO_2 can take part in chemical reactions such as the formation of carbonic acid:

$$H_2O + CO_2 \leftrightarrow H + HCO_3^- \leftrightarrow H_2CO_3$$

Once formed, the carbonic acid (H_2CO_3) can cause weathering of rocks. Several biological processes involve CO_2, including methanogenesis:

$$CO_2 + 4H_2 \rightarrow CH_4 + 2H_2O$$

denitrification:

$$5CH_2O + 4H^+ + 4NO_3^- \rightarrow 2N_2 + 5\,CO_2 + 7H_2O$$

fermentation:

$$C_6H_{12}O_6 + 4N_2 + 7H_2O \rightarrow 6CO_2 + 8NH_3$$

and aerobic respiration:

$$CH_2O + O_2 \rightarrow CO_2 + H_2O$$

Because of the broad range of involvement CO_2 has with other biogeochemical processes and the gas and liquid phase transport via advection and diffusion, soil CO_2 and respiration fluxes are likely decoupled under certain conditions (Sánchez-Cañete et al., 2018). To address this issue, simultaneous soil CO_2 and O_2 measurements have been proposed to improve the understanding of and to discriminate between biotic and abiotic controls on soil CO_2 dynamics (Angert et al., 2015; Hicks Pries et al., 2019; Sánchez-Cañete et al., 2018).

Alone, O_2 is an important compound that influences biogeochemistry (Silver et al., 1999). For instance, the presence of O_2 not only determines aerobic-anaerobic conditions but also influences redox potentials (Patrick & Jugsujinda, 1992), and availability of nutrients (Pett-Ridge et al., 2006; Rubol et al., 2012; Silver et al., 1994). O_2 is the most energetically favorable substance for metabolism. In anaerobic conditions, less energetically favorable substances like N_2, NO_3, or sulfate (SO_4) will be used for metabolism, as determined by the standard reduction potential of the substance. Denitrification, for example, has a redox potential of 0.749 V, while sulfide oxidation has

a redox potential of -0.222 V; therefore, NO_3 is a more energetically favorable electron acceptor. High rates of denitrification have been correlated to high water saturation, creating low O_2 availability, as well as the temporal extent of anoxic and aerobic conditions (Schlüter et al., 2019). The increase of denitrification is linked to the frequently changing aerobic and anoxic conditions (Reddy & Patrick, 1975). Due to the fluctuations of precipitation, aerobic and anaerobic conditions can be extremely variable, often creating an aerobic-anaerobic process continuum. The variability in redox affects the structure and biomass of the microbial communities in which high variability of redox supports both aerobic and anaerobic microbes (Deangelis et al., 2012; Pett-Ridge et al., 2006).

Soil metabolism is of interest due to the biological role in nutrient uptake as well as carbon cycling. Soil respiration is the sum of heterotrophic and autotrophic respiration that occurs within the soil. By monitoring soil respiration at the same time as hydrologic conditions, the driving forces of soil biotic and abiotic activity can be analyzed (Raich & Schlesinger, 1992). Additionally, the trigger of biological metabolism may be identifiable, given the gas concentrations and soil hydrologic conditions.

2.5 Biogeochemical Process Interpretation

Soil biogeochemical processes, specifically microbial respiration, may be identified when analyzing CO_2 and O_2 gas concentrations simultaneously. For example, aerobic respiration stoichiometry predicts microbes and roots produce one mole of CO_2 for every mole of O_2 they consume. The apparent respiratory quotient (ARQ) is defined as the ratio of the soil CO_2 efflux to the O_2 influx (Angert et al., 2015; Angert & Sherer,

2011; Ferraz de Almeida et al., 2018; Hicks Pries et al., 2018). Therefore, aerobic respiration theoretically has an equal molar concentration of O_2 intake to CO_2 produced based on a stoichiometric equation. Coupling CO_2 and O_2 measurement can potentially distinguish other biogeochemical processes as well (Hodges et al., 2019).

When trying to identify which process is related to gas production or usage, there is much difficulty in separating the biological and geochemical carbon contributions (Amundson et al., 2007). If gas concentrations are simultaneously analyzed, then the identification of the process is narrowed down. Based on stoichiometric equations of the biogeochemical process, the abiotic and biotic processes can be distinguished from coupled CO_2 and O_2 measurements (see Table 1). Abiotic processes like oxidation of Fe, Mn, S, and NH_4; weathering of silicate and carbonate; and CO_2 dissolution all result in either CO_2 or O_2 consumed. Meanwhile, aerobic biological activity results in O_2 consumed and CO_2 produced. Anaerobic respiration results in CO_2 produced but no O_2 consumed, thus resulting in a higher ratio than aerobic respiration because the difference in CO_2 is relatively larger than the O_2 difference. There are exceptions such as anaerobic biological process, methanogenesis, which can use CO_2 instead of acetic acid for the electron acceptor, thus resulting in a ratio of -1:0. Once the processes are identified with their corresponding CO_2:O_2 stoichiometry, tracking the activity in response to variable conditions is then possible.

Table 1: *Biogeochemical reactions in soil, with CO_2:O_2 ratios that can help distinguish abiotic from biotic processes.*

Biogeochemical Process	***Reaction***	***CO_2:O_2 Ratio***
Oxidation (i.e., Fe^{2+})	$4Fe^{2+} + O_2 + 4H_2O \rightarrow 2Fe_2O_3 + 8H^+$	0:1
Silicate Weathering	$CaSiO_3 + CO_2 \rightarrow CaCO_3 + SiO_2$	1:0
Carbonate Weathering	$CaCO_3 + CO_2 + H_2O \rightarrow Ca^{2+} + 2HCO_3^-$	1:0
CO_2 Dissolution	$CO_2 + H_2O \rightarrow H^+ + CO_3^{2-}$	1:0
Aerobic Methane Oxidation	$CH_4 + 2O_2 \rightarrow CO_2 + 2H^+$	1:2
Aerobic Respiration	$CH_2O + O_2 \rightarrow CO_2 + H_2O$	1:1
Anaerobic Respiration (i.e., sulfate reduction)	$2CH_2O + 2H^+ + SO_4^{2+} \rightarrow H_2S + CO_2 + 2H_2O$	1:0

2.6 Recap: Research Objectives

This study has two main objectives:

Objective 1: Determine if soil moisture and/or temperature can predict the apparent respiratory quotient (ARQ).

Question: Are soil moisture and/or temperature able to predict the ARQ?

Objective 2: Run model simulations of soil gas advection, diffusion, and reactions and their response to soil moisture to test if the temporal variability in ARQ is driven by physical or biogeochemical processes.

Question: Can we infer what biogeochemical process is occurring using the ARQ values?

3. METHODS

3.1 Field Sites

To monitor the biogeochemical activity response to hydro-climatic conditions, sensors were deployed in soils at several GSI sites in Milwaukee, Wisconsin. The sensors were the Apogee model SO-110 oxygen and temperature sensor, the Eosense EosGP carbon dioxide sensor, and the Campbell Scientific CS650 water content reflectometer. The SO-110 uses galvanic cells to sense O_2 concentrations and was calibrated using the ambient air before installation. The O_2 concentrations reported were within an accuracy of ± 0.1% and drift by 1 mV per year. The EosGP sensor used optical electrodes to sense CO_2 concentration and was calibrated in two ranges, 0 to 1,000 ppm and 0 to 20,000 ppm. The higher CO_2 calibrated range was used in the reported results. The Eosense EosGP had an accuracy of ± 1% of recorded CO_2 concentrations. The CS650 utilized a time domain reflectometer to obtain volumetric water content (VWC) readings in units of m^3m^{-3}. Reported VWC readings had an accuracy of ± 3%. Sensors were placed 15 cm beneath the soil surface and were connected to a CR1000 or CR300 datalogger. The dataloggers were powered by either connection to the electrical grid or a Campbell Scientific 12V, 24 amp hour, sealed rechargeable lithium ion battery supplying a steady 12V power supply. At the sites with a battery, the battery was charged and replaced every week to ensure the charge stayed above the power limit required by the sensors. All dataloggers, power converters, and open wires were protected by a field enclosure. Data was collected at a frequency of 5 minutes. Each sensor was calibrated before deployment following protocols set by the manufacturers.

Data collected include sensor measured soil O_2, CO_2, VWC, and temperature at four field sites. It should be noted that the results presented here exclude CO_2 readings that were sporadically at zero. The manufacturers of the sensor, Eosense, and datalogger, Campbell Scientific, explained that these occasional zero readings were due to the logger or inability of the sensor to sample the CO_2 or log the reading at the high frequency of every 5 minutes. Additionally, each sensor had a specific concentration range at which they were able to detect. For CO_2 sensors deployed in this study the upper limit was 40,000 ppm, which was reached at some of the sites. At these instances, the sensor read a negative zero, and these readings were ignored for the analysis. None of the sites were irrigated during the collection periods. Precipitation data was obtained from General Mitchell International Airport station which was approximately six to eight miles from the GSI sites.

One site was an urban garden known as the Victory Garden located by Weasler Auditorium at Marquette University (Figure 1). The plots were raised beds that were held in by 2”x4” boards around the perimeter. At this site, two sets of the sensors were deployed at a western plot in July 2018. On April 2019, one set of sensors was moved to an eastern plot. Once the growing season began the western plot grew squash while the eastern plot grew beans. The media was a type of silty loam potting soil for approximately 30 cm deep. The plots were not shaded by trees or buildings, but a single-story building, Weasler Auditorium, was located about 3.5 meters to the north of the plots.

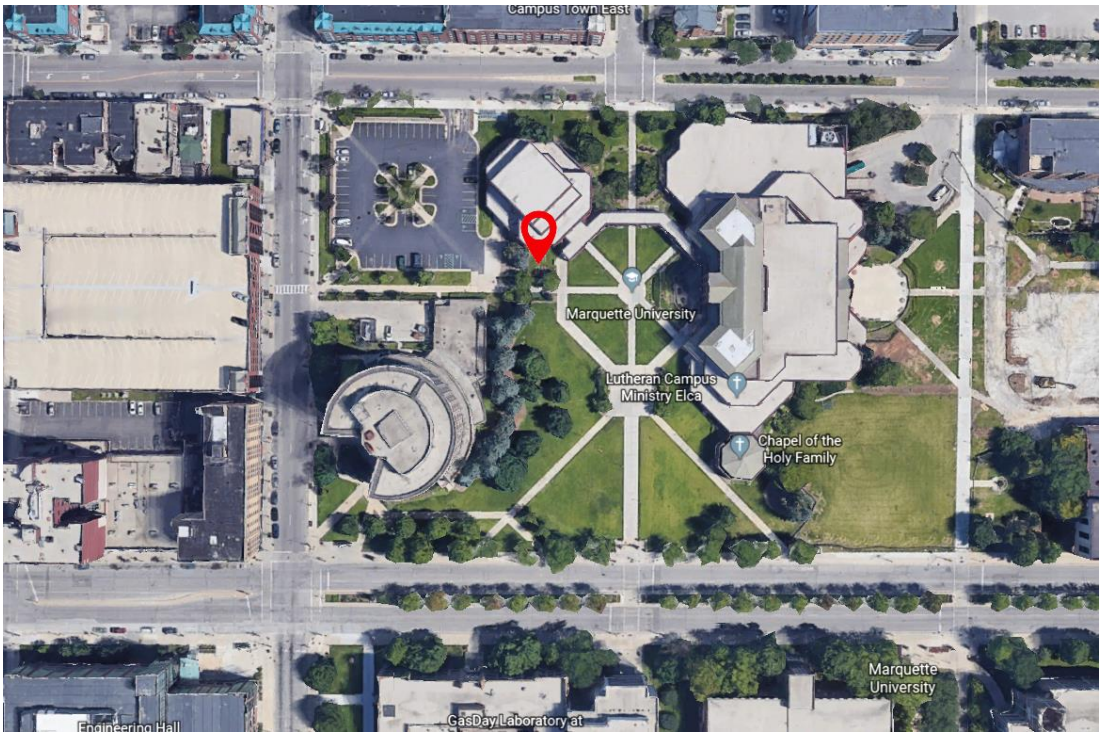

Figure 1: Victory Garden plots at Marquette University. Map source: ESRI, DigitalGlobe, Earthstar Geographics, CNES/Airbus DS, USDA, AeroGRID, IGN, and the GIS User Community.

The second site was the green roof which was also located on Marquette University campus on the second story balcony of the four-story Engineering Hall (Figure 2). Power was supplied by the 30 solar panels on the balcony of the building. The green roof was located on the southside of the building. The media was a gravel-like substance and was approximately 20 cm deep. The majority of the plant species present were succulents and some other species like milkweed, clover, and grasses. The green roof has two drains to remove excess precipitation in the case of large events. One set of sensors were deployed as far as possible from the drains and ledge of the green roof. Plastic corrugated piping protected the cables between the datalogger encasement and the sensors to avoid damage.

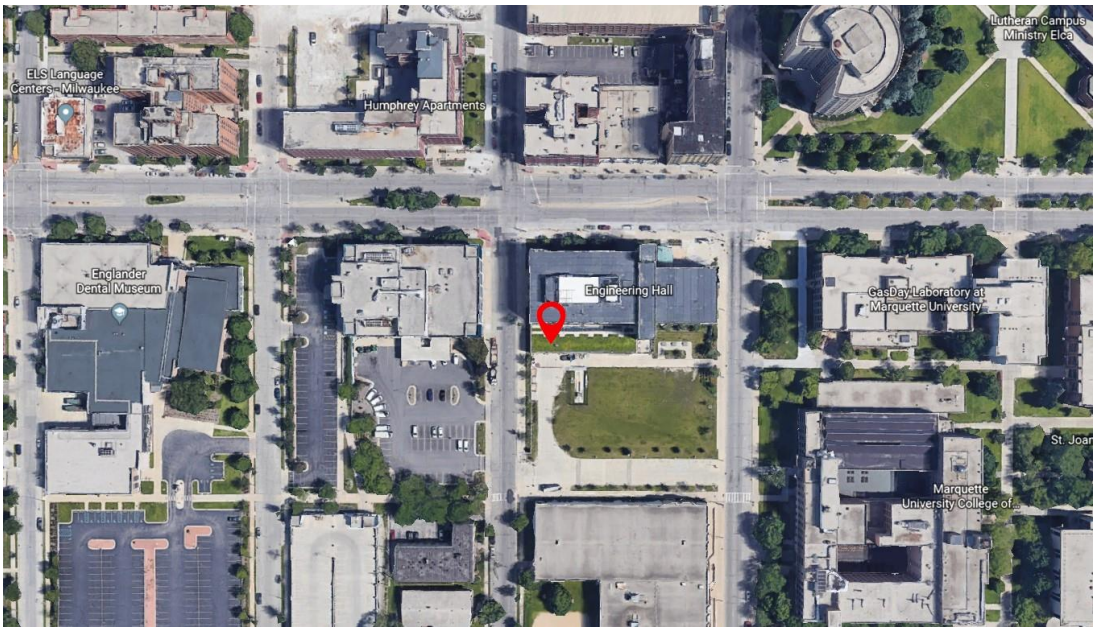

Figure 2: Green roof on Marquette University Engineering Hall. Map source: ESRI, DigitalGlobe, Earthstar Geographics, CNES/Airbus DS, USDA, AeroGRID, IGN, and the GIS User Community.

The third site was a wetland located at the Milwaukee Metropolitan Sewer District (MMSD) Headquarters in Milwaukee Wisconsin (Figure 3). The ~670 m^2 wetland generally had standing water in it, but the sensors were placed upland in the drier section due to cord length restrictions. The media observed at the site was a silty-loam type soil and did not appear to have a depth restricted by a liner. The soil moisture sensor used at this site was the Sentek Drill and Drop soil moisture profiler, while the CO_2 and O_2 sensors were the same as the other sites. The sensors were powered by one of the rechargeable batteries. The Menomonee River was approximately 68 meters west from the deployed sensors.

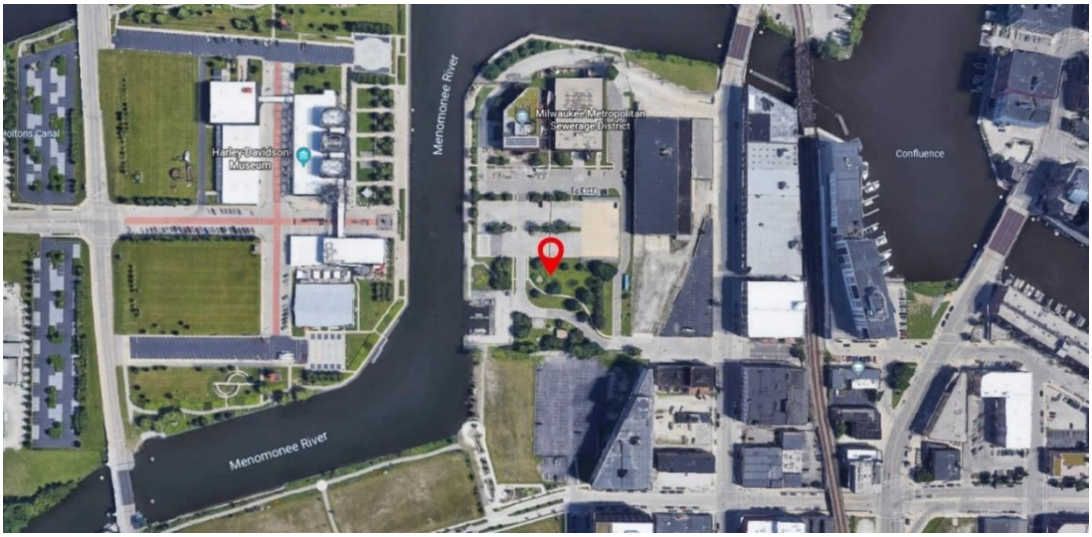

Figure 3: Wetland at MMSD location. Map source: ESRI, DigitalGlobe, Earthstar Geographics, CNES/Airbus DS, USDA, AeroGRID, IGN, and the GIS User Community.

The final site was the wetland at Three Bridges Park off 35th street in Milwaukee Wisconsin (Figure 4). This wetland was approximately 9,100 m^2 in area (Table 2). At this location, two sets of sensors were deployed, one upslope and one downslope near the standing water about 3 meters from one another. The upland plot was approximately one meter higher in elevation from the lowland plot. The media observed at this site was a silty-clay type soil in the upland plot and a silty-sand type soil in the lower location. Similar to the wetland at MMSD, this site did not appear to have a liner restricting the media depth. The Menomonee River was about 90 meters southeast of the sensors. This wetland was different from the wetland at MMSD headquarters because this site consists of a system of connected wetlands in which during large storm events the monitored wetland flows into an adjacent wetland closer to the Menomonee River. See Table 2 for a comprehensive overview and additional information of the four locations.

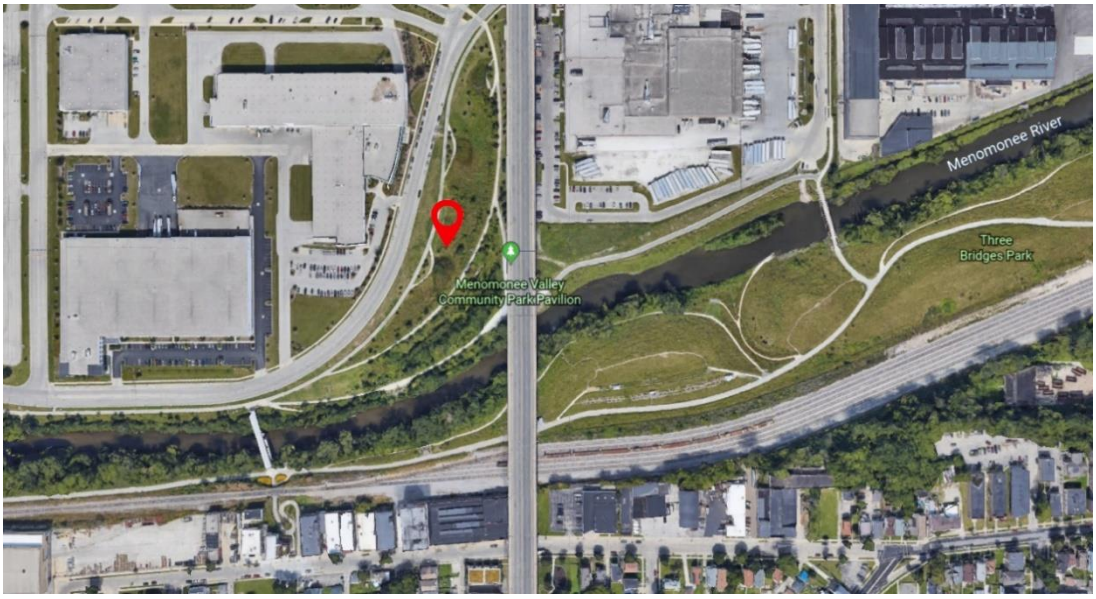

Figure 4: Location of the sensors deployed at the Three Bridges Park wetland. Map source: ESRI, DigitalGlobe, Earthstar Geographics, CNES/Airbus DS, USDA, AeroGRID, IGN, and the GIS User Community.

Table 2. *List of monitoring sites and their location, size, and additional descriptive information.*

Type of Infrastructure	**Location**	**Size**	**Additional Information**
Urban Garden	Marquette University	2.7 m^2/plot	Data collected from two growing seasons
Green Roof	Marquette University	387 m^2	Soil type and depth were uniquely different from the other GSI sites
Wetland	MMSD Headquarters	670 m^2	Single wetland
Wetland	Three Bridges Park	9100 m^2	Wetland system, two collection locations – upland and lowland

3.2 Apparent Respiration Quotient

The soil CO_2 and O_2 data were used to calculate the apparent respiratory quotient (ARQ) (Angert et al., 2015; Angert & Sherer, 2011). ARQ is defined as the ratio between the soil CO_2 efflux to O_2 influx and serves as a way to categorize the chemical, biological, and physical soil activities (Ferraz de Almeida et al., 2018). The ARQ considers the physical transport of the gases by diffusion and the changes of the gases caused by biogeochemistry. Angert et al. (2015) and Hicks Pries et al. (2019) defined ARQ as:

$$ARQ = -\frac{D_{CO_2}}{D_{O_2}}\frac{\Delta CO_2}{\Delta O_2}. \quad (1)$$

The ratio of the diffusivities of the gases in air ($D_{CO_2}/\ D_{O_2}$) at standard temperature and pressure is 0.76. The change of the gases (ΔCO_2 and ΔO_2) is the difference between the soil concentration and the atmospheric concentration. The difference in O_2 concentrations is negative because the source of O_2 is the atmosphere and O_2 is depleted in the soil.

The ARQ values indicate different biogeochemical processes that are occurring, such as the ones listed in Chapter 2.4 and Table 1 of Chapter 2.5. Aerobic respiration has an ARQ of 0.76, indicating an equivalent O_2 consumption to CO_2 production. ARQ values that differ from 0.76 represent an imbalance of O_2 influxes and CO_2 effluxes relative to aerobic respiration. For example, during methane oxidation, two O_2 molecules are consumed and a mole of CO_2 is consumed to produce methane (CH_4) which results in an ARQ of 0.38. Likewise, oxidation reactions such as iron oxidation ($4Fe + 3O_2 \rightarrow 2Fe_2O_3$) result in a lower ARQ value because three moles of O_2 are consumed and no

CO_2 is produced. When anaerobic activities like denitrification or fermentation occur, no O_2 is consumed while CO_2 is produced from carbon sources like methanol or glucose, producing an ARQ value higher than 0.76. The calculated ARQ values provide a frame of reference to begin to understand what biogeochemical process is dominant in the soil.

3.3 Statistical Analysis

Statistical analyses were performed using the MATLAB linear regression function. The correlation analysis was used to determine whether ARQ or O_2 were related to soil temperature or VWC to justify if either soil condition could predict the soil activity. To measure the goodness of fit the r^2 was calculated. A t-test was also conducted to check the significance of the linear fit, with $p<0.05$ signifying significance.

3.4 Advection-Diffusion-Reaction Model with Soil Moisture

To evaluate the control of VWC and soil temperature on ARQ, simulations were conducted with an advection-diffusion-reaction model. The model simulated the VWC (θ_w), CO_2, and O_2 transport through a soil profile. The soil moisture dynamics, $\theta_w(z,t)$, were simulated using a head-based formulation of Richards Equation, solved using a Picard iteration scheme (Celia & Bouloutas, 1990). Richards equation also included evaporation, transpiration, and water stress in the soil moisture transport. Evaporation was based on the soil moisture at the surface of the profile at a maximum rate of 1.125 mm/day. Transpiration by the plants occurred at a maximum rate of 3.375 mm/day. In the case of soil moisture deficiency, plants will try to limit water loss through leaves by closing the stomatal openings thus restricting photosynthesis and other plant activities.

Therefore, additional parameters included were incipient stress at 0.263/porosity and wilting stress at 0.075/porosity which results in partial and complete stomatal closure, respectively. The top boundary condition was allowed to switch between a constant flux, associated with the precipitation or evaporation rates, and a constant head under ponding conditions (Salvucci & Entekhabi, 1995). The bottom boundary condition was specified as free drainage. The modelled water transport was impacted not only by precipitation and soil physical properties but also by plant activity.

Table 3: *List of sources and transport of the model variables.*

Model Parameters	***Source***	***Transport***
VWC (θ_w)	Precipitation	Evaporation Transpiration Infiltration
CO_2	Soil Respiration	Advection Diffusion
O_2	Soil Respiration (sink)	Advection Diffusion

For both gases, the top boundary condition was specified as a constant concentration equal to the atmospheric concentration, and the bottom boundary condition was specified as a natural outflow. CO_2 and O_2 transport were driven by diffusion and advection fluxes. The O_2 source is from the atmosphere which was set to a concentration of 209,500 ppm. CO_2 is sourced from the soil and diffuses upward to the atmosphere, and was set to 406.58 ppm based on the concentration measured in June 2019 at the NOAA Mauna Loa Observatory, Hawaii (Earth System Research Laboratory, 2019). Diffusive flux moves the gases from higher concentration in the soil or atmosphere to an area of lower concentration and is limited by pore space filled with water. The model represented

advection of gases as influenced by the water velocity. The focus of the model simulations was the effect of moisture transport on ARQ variability within a single season and, therefore, the model only simulated θ_w and not temperature.

The one-dimensional, vertically resolved mass balance equations for the gas phase concentrations of CO_2 and O_2 were as follows:

$$\frac{\partial \theta_a R_f [CO_2]}{\partial t} = \frac{\partial}{\partial z}\left[\theta_a D_{CO_2}(\theta_w)\frac{\partial [CO_2]}{\partial z} - q[CO_2]\right] - T(\theta_w)K_{H,c}[CO_2] + R_{CO_2}(\theta_w) \quad (2a)$$

$$\frac{\partial \theta_a R_f [O_2]}{\partial t} = \frac{\partial}{\partial z}\left[\theta_a D_{O_2}(\theta_w)\frac{\partial [O_2]}{\partial z} - q[O_2]\right] - T(\theta_w)K_{H,o}[O_2] - R_{O_2}(\theta_w) \quad (2b)$$

where soil respiration (R) and diffusivity (D) were assumed to be functions of θ_w, $\theta_a = n - \theta_w$ is the volumetric air content, $q = q_a + K_H q_w$ is the effective velocity that accounts for the gas velocity q_a and water velocity q_w, T is the transpiration rate, and $R_f = 1 + \frac{K_H \theta_w}{\theta_a}$ is a retardation coefficient that accounts for dissolution of the gases. Dissolution was modeled as an equilibrium process following Henry's Law with dimensionless coefficient, K_H. In addition to the set of equations (2), it was assumed gases instantly fill the available pore spaces in relation to water volume changes, leading to the following additional constraint (Simunek & Suarez, 1993),

$$q_a = q_w(L) - q_w + \int_z^L T dz \quad (3)$$

where L is the soil depth. The vertical root profile was assumed to follow an exponential shape with a mean depth, z_r. The system of equations (2) and (3) were solved using an explicit finite volume scheme with first-order approximations of the diffusive and advective fluxes.

Biogeochemical processes were represented by α which was the assumed stoichiometry of respiration, equivalent to the ratio $\frac{R_{CO_2}(\theta_w)}{R_{O_2}(\theta_w)}$. The model assumed α increased linearly with VWC where $\alpha = \theta_w/n$ and n is the porosity of the soil. The variable α can take any value between 0 and 1. Some baseline examples based on theoretical stoichiometric relationships are that for biological respiration, α = 1, and for methane oxidation, α = 0.5. Additionally, the diffusivity (mm^2/s) was assumed to be a function of VWC i.e.,

$D(\theta_w) = (n-\theta)D_{atm} + K_H D_{atm}\theta_w \left[\frac{(n-\theta_w)^{\frac{10}{3}}}{n^2}\right]$ (Moyano et al., 2013; Simunek & Suarez, 1993). With these assumptions both physical (diffusivity) and biogeochemical processes (respiration stoichiometry) are influenced by VWC.

3.4.1 Simulations

The model simulations were designed to determine whether the ARQ variability is due to physical or biogeochemical processes. From equation (1), ARQ considers the diffusivities of the gases and changes in the gas concentrations due to biogeochemical sources or sinks and it is related to the modeled α parmater in the following way:

$$ARQ(\theta_w) = \frac{D_{CO_2}(\theta_w)}{D_{O_2}(\theta_w)}\frac{\Delta CO_2}{\Delta O_2} = \frac{R_{CO_2}(\theta_w)}{R_{O_2}(\theta_w)} = \alpha(\theta_w). \quad (4)$$

Therefore, ARQ can vary with increased θ_w through one of two means: reduction of diffusivity (physical) or increase in ARQ (biogeochemical). The model simulations used to discriminate between these two means were as follows:

1. α and VWC were set as constant – control simulation, neither physical nor biogeochemical processes influent gas dynamics;
2. α was constant and VWC was variable – physical processes only influence gas dynamics; and
3. α and VWC were variable – biogeochemical and physical processes influence gas dynamics.

For the variable VWC simulations, the model was forced with 30-year hourly rainfall data from NOAA.

3.5 CO_2 – O_2 Phase Space Analysis

Visualizing the soil gas system in the CO_2-O_2 phase space provides insight into the active soil biogeochemical processes (Romanak et al., 2012). Theoretical relationships between CO_2 and O_2 were derived from equation (4) in which O_2 can be written as a function of soil CO_2,

$$[O_2] = [O_2]_{atm} - \frac{D_C}{\alpha D_O}([CO_2]_{atm} - [CO_2]) \quad (5)$$

where $[O_2]_{atm}$ and $[CO_2]_{atm}$ are the atmospheric gas concentrations, which were assumed to be constant. Analyzing the CO_2-O_2 phase space can further identify the abiotic processes. Deviations of CO_2-O_2 readings below the stoichiometric aerobic respiration can be due to a reduction in CO_2 (i.e. CO_2 dissolution) or reduction in O_2 (i.e. oxidation reactions) (Hodges et al., 2019). CO_2-O_2 phase space analysis can assist with visualizing these deviations.

4. RESULTS

4.1 Field Results

The field data results are organized below by site in the following order: Victory Garden plot 2018, Victory Garden West plot, Victory Garden East plot, green roof, MMSD wetland, Three Bridges Park wetland lowland plot, and Three Bridges Park wetland upland plot.

4.1.1 Victory Garden Field Results From 2018

In 2018 (July 7- September 30), the soil temperature, O_2, and CO_2 all fluctuated on a daily scale and soil VWC fluctuated in response to precipitation events. The O_2 was lowest in September at 16% and remained consistently above 18% in July and August of 2018 (Figure 5a). The CO_2 remained below 10,000 ppm from July until the end of August (Figure 5b). In September, the CO_2 increased above 20,000 ppm then decreased to 10,000 ppm for the remainder of the month (Figure 5b). Soil temperature generally remained between 20 and 25 °C until mid-September when the temperature decreased (Figure 5d). The VWC was low in the summer months from mid-July to August in which the soil moisture fell below 20%. The VWC did not respond strongly to precipitation events in July and August potentially because the events did not result in much infiltration due to increased canopy interception during the growing season or the field site did not receive the same amount of precipitation that the rain gage at the Milwaukee airport received. There were several rain events from the end of August through the

beginning of September that resulted in the soil VWC increasing to above 40% (Figure 5c).

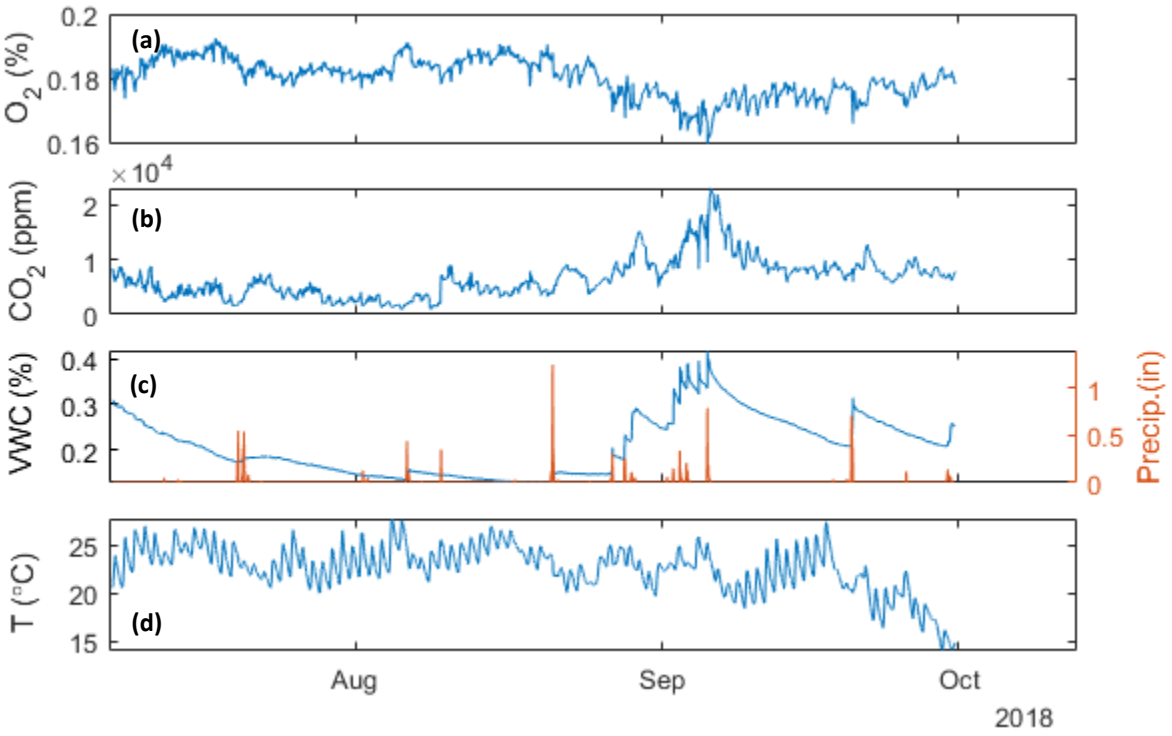

Figure 5. Timeseries of O_2 (a), CO_2 (b), VWC ($m^3\ m^{-3}$) and precipitation (c) and soil temperature (d) at 15 cm deep in the Victory Garden West plot from July 7 to September 30, 2018.

Linear regression suggested O_2 relationship to soil temperature was not strongly linear with a reported r^2 of 8% but the relationship was significant ($p<0.05$, Figure 6a). Meanwhile, soil O_2 concentrations decreased with VWC. Linear regressions showed soil VWC explained 51% of the O_2 variability and the relationship was significant ($p<0.05$, Figure 6b). However, the linear model did not best represent the relationship between O_2 and temperature as lower temperatures appear to have a negative relationship with O_2 (Figure 6a).

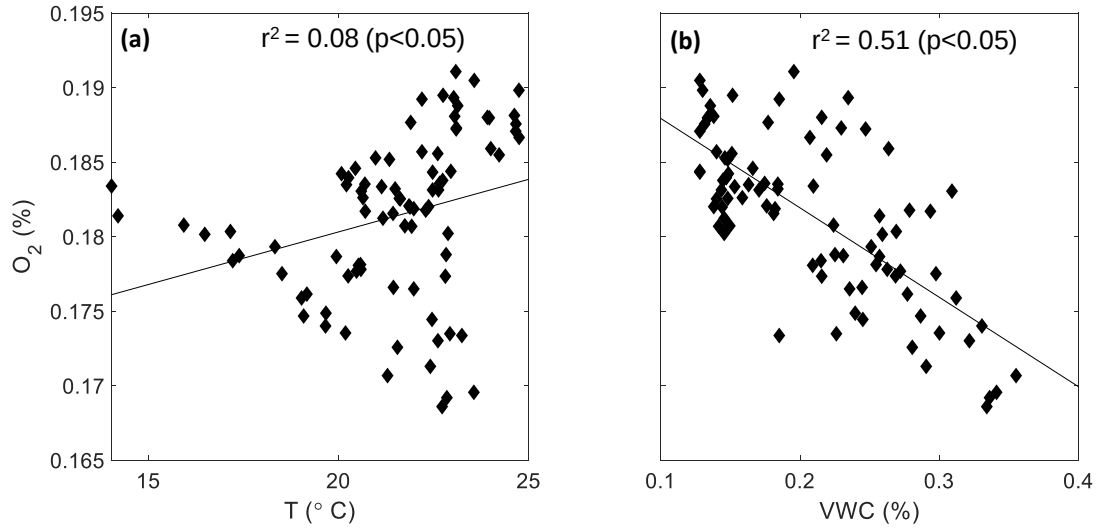

Figure 6. Correlation between daily O_2 and soil temperature (a) and soil moisture (b) at the Victory Garden West plot for July 7 through September 30, 2018. The black line corresponds to the linear regression line.

The ARQ variability was explained more by VWC than by temperature at the Victory Garden West plot in 2018. The linear regression suggested the response of ARQ to soil temperature was not strongly linear with a reported r^2 of 6%, although the relationship was significant ($p<0.05$, Figure 7a). ARQ increased with VWC. Linear regression showed VWC explained 41% of ARQ variability and the relationship was significant ($p<0.05$, Figure 7b).

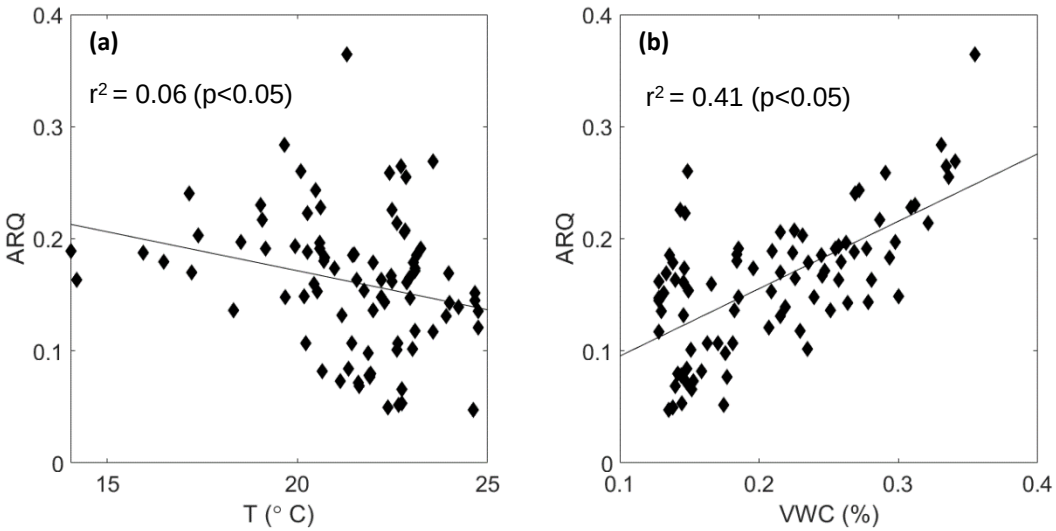

Figure 7. Correlation between daily ARQ and soil temperature (a) and soil moisture (b) at the Victory Garden West for July 7 through September 30, 2018. The black line corresponds to the linear regression line.

4.1.2 Victory Garden West Plot 2019 Field Data Results

At the Victory Garden West plot in 2019 (March 29 – October 17), the soil temperature, O_2, and CO_2 all fluctuated on a daily scale and soil VWC fluctuated in response to precipitation events. The soil O_2 varied between 14 and 18% (Figure 8a). The lowest O_2 concentration occurred in the beginning of July which then increased to nearly 18% within nine days (Figure 8a). CO_2 ranged from 645 ppm to 26,280 ppm over the seven-month collection period (Figure 8b). Soil moisture was highest from May through June while the driest period was experienced between August through September 10, despite the nearly weekly precipitation events that occurred in that period (Figure 8c). Soil temperature in the Victory Garden West plot gradually increased from April to July then decreased from August to the end of the project in October (Figure 8d). Daily soil temperature varied greatly from April until July then was less variable on a diurnal time scale through to the end of the collection period (Figure 8d).

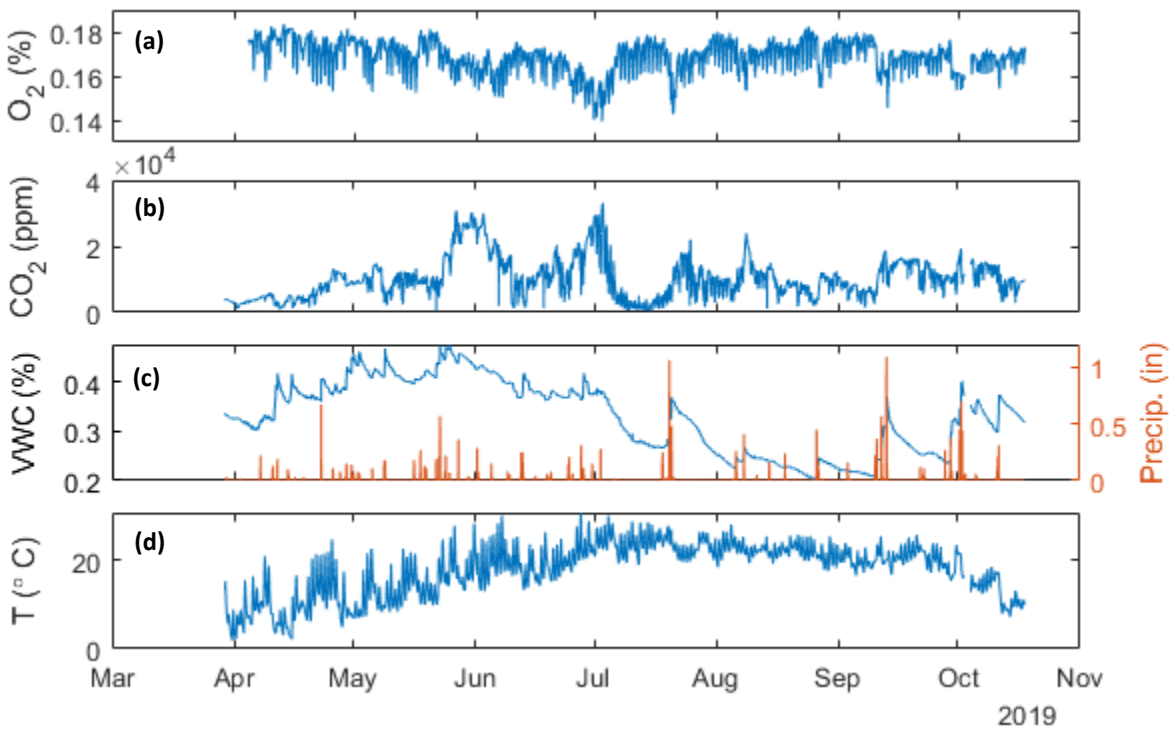

Figure 8. Timeseries of O_2 (a), CO_2 (b) VWC and precipitation (c) and soil temperature (d) at 15 cm deep in the Victory Garden West plot during March 29 – October 17, 2019.

Soil O_2 concentrations decreased with soil temperature and VWC. Linear regressions showed temperature explained 27% of O_2 variability (Figure 9a), while VWC explained 8% of O_2 variability (Figure 9b). Both relationships were significant ($p<0.05$).

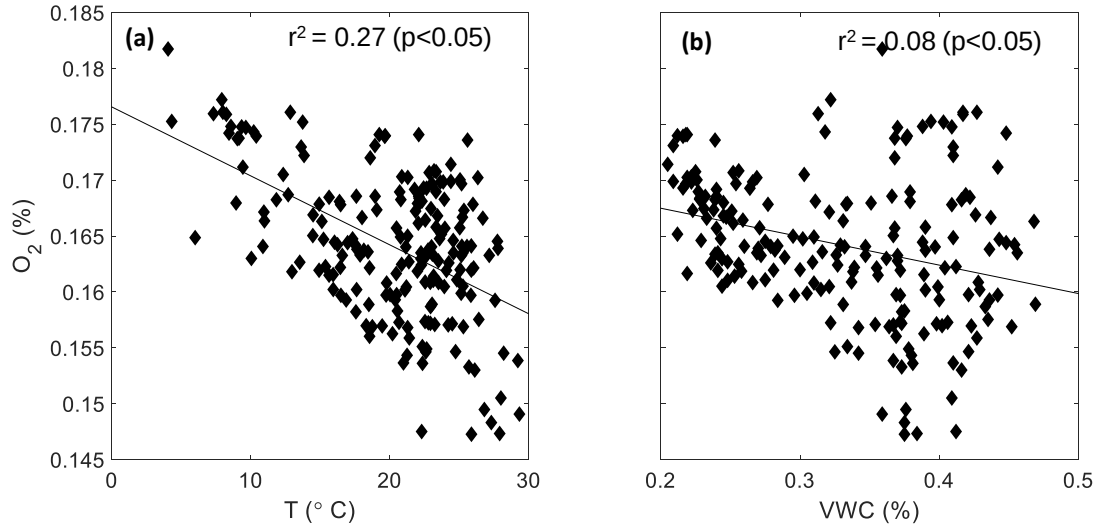

Figure 9. Correlation between daily O_2 and soil temperature (a) and soil moisture (b) at the Victory Garden West plot for March 29 through October 17, 2019. The black line corresponds to the linear regression line.

More ARQ variability was explained by VWC than by soil temperature at the Victory Garden West plot in 2019. Linear regression analysis on the relationship between ARQ and temperature resulted in an r^2 of 0.06% and the relationship was not significant ($p>0.05$, Figure 10a). ARQ increased with VWC. Linear regression showed VWC explained 11% of ARQ variability and the relationship was significantly ($p<0.05$, Figure 10b). Interestingly, the same plot in 2018 (July 7- September 30) had ARQ variability significantly explained by both soil temperature and VWC by 6% and 41%, respectively. Based on the Victory Garden West plot data, the linear relationships differ between the two years.

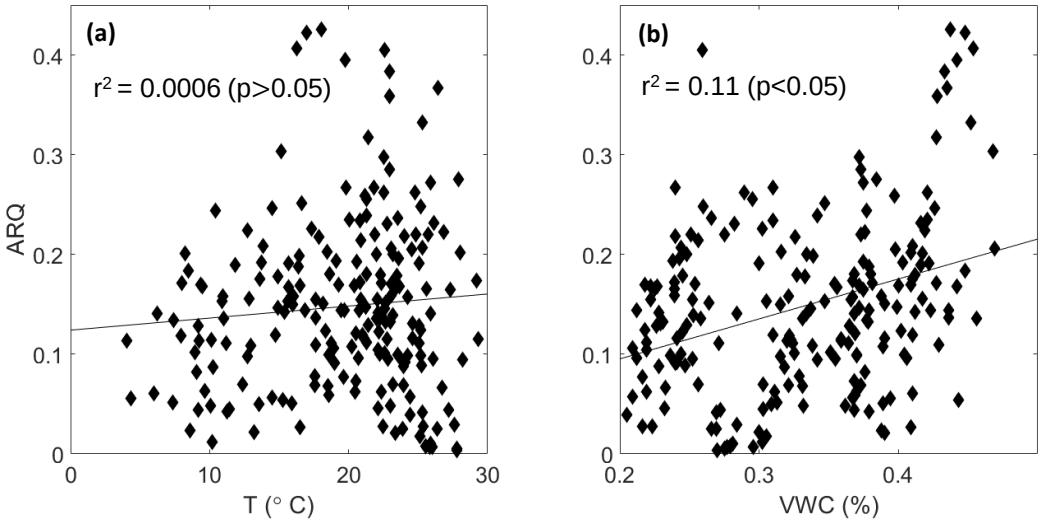

Figure 10. Correlation between daily ARQ and soil temperature (a) and soil moisture (b) at the Victory Garden West plot for March 29 through October 17, 2019. The black line corresponds to the linear regression line.

4.1.3 Victory Garden East Plot Field Data Results

In the Victory Garden East plot in 2019, the soil temperature, O_2, and CO_2 fluctuated on a daily scale and soil VWC fluctuated in response to precipitation events. The O_2 concentration varied between 16% on July 20 and 20% on April 27 (Figure 11a), while CO_2 varied between 1,143 ppm on August 25 and 23,393 ppm on July 21 (Figure 11b). Soil moisture was higher in the months of May and October while the driest period was from mid-July through the beginning of September (Figure 11c). In general, soil temperature increased from the end of March to July then decreased from August to the middle of October (Figure 11d).

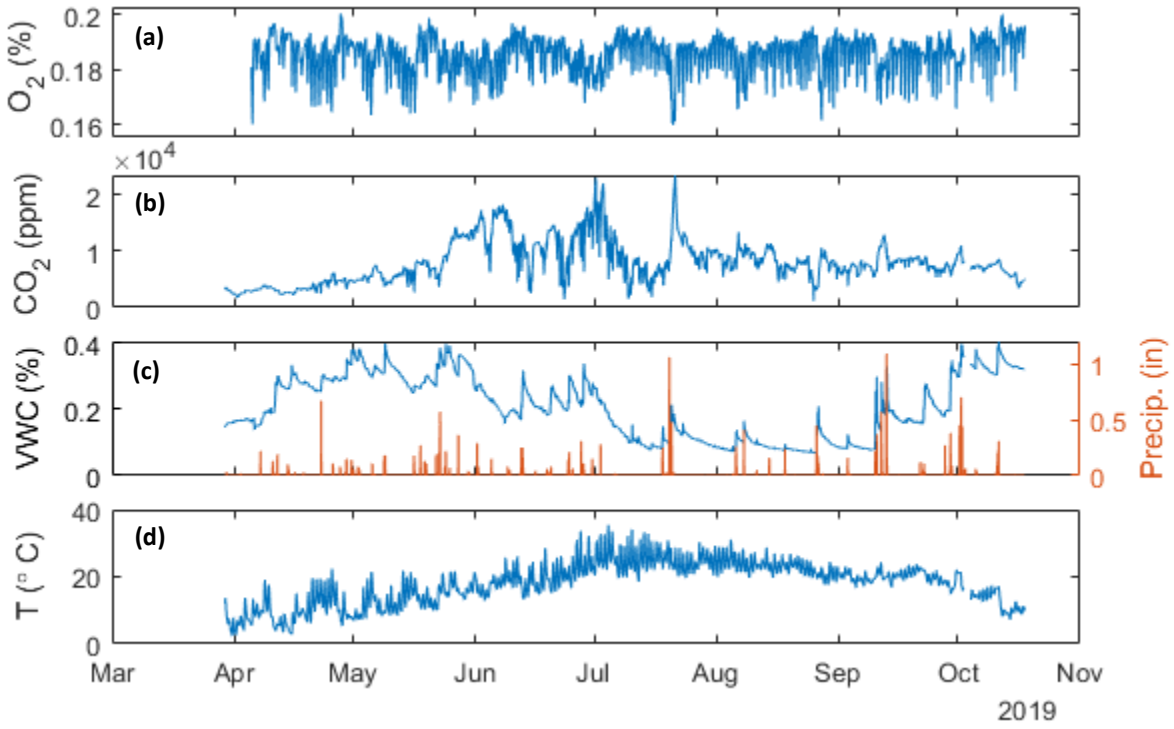

Figure 11. Timeseries of O_2 (a), CO_2 (b), VWC and precipitation (c) and soil temperature (d) at 15 cm deep in the Victory Garden East plot during March 29 – October 17, 2019.

Soil O_2 concentrations decreased with soil temperature but did not vary with VWC. However, linear regression suggested the O_2 response to soil temperature was not strongly linear with a reported r^2 of 4%, but the relation was significant ($p<0.05$, Figure 12a). O_2 did not vary with VWC. Linear regression analysis of the relationship between O_2 and VWC resulted in an r^2 of 0.2% and the relationship was not significant ($p>0.05$, Figure 12b).

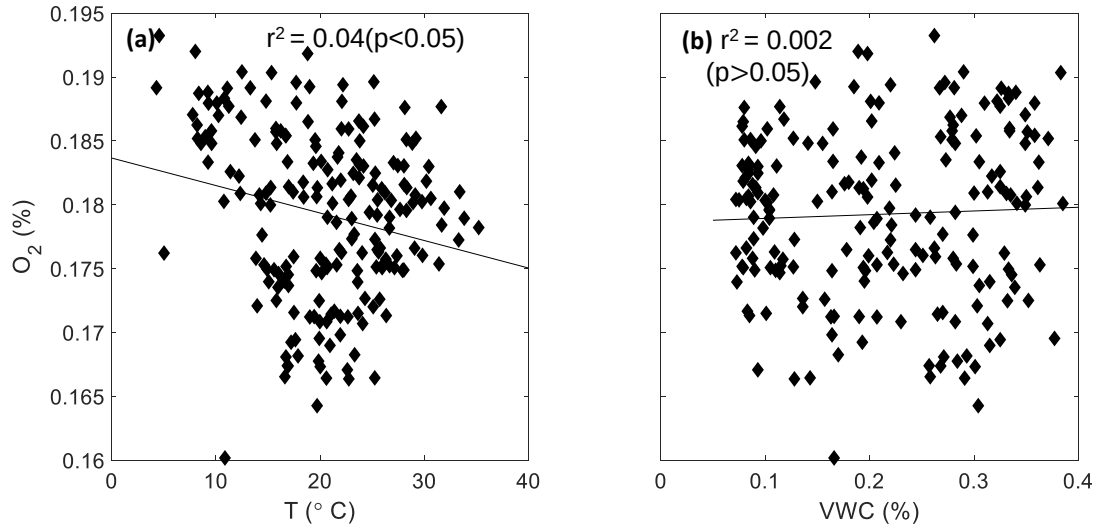

Figure 12. Correlation between daily O_2 and soil temperature (a) and soil moisture (b) at the Victory Garden East plot for March 29 through October 17, 2019. The black line corresponds to the linear regression line.

The ARQ variability was explained more by temperature than by VWC at the Victory Garden East plot in 2019. ARQ increased with soil temperature. However, linear regression suggested the ARQ response to soil temperature was not strongly linear with a reported r^2 of 8%, although the relationship was significant ($p<0.05$, Figure 13a). ARQ was also not strongly related to VWC in the Victory Garden East plot in 2019. VWC did not show a significant linear relation with ARQ, with an r^2 of 0.1% ($p>0.05$ Figure 13b).

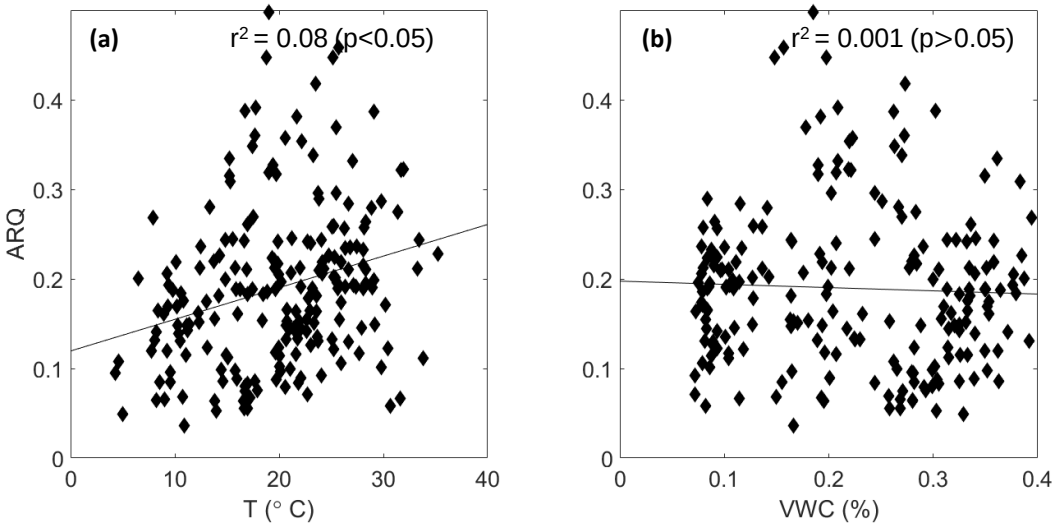

Figure 13. Correlation between daily ARQ and soil temperature (a) and soil moisture (b) at the Victory Garden East plot for March 29 through October 17, 2019. The black line corresponds to the linear regression line.

4.1.3.a Comparison Between 2018 and 2019 Victory Garden Data

The comparison between the years 2018 and 2019 for the period of July 7 to September 30 at the Victory Garden West plot showed differences in both VWC and ARQ values (Figure 14). The 75th percentile of the VWC distribution in 2018 was 36% and in 2019 it was 26%. The median VWC in 2018 was 21% and in 2019 it was 18%. The temperature medians were similar in 2018 and 2019. The ARQ median in 2018 was 0.16 and in 2019 it was 0.24. In general, during this time period, 2019 was drier and saw higher ARQ values than in 2018.

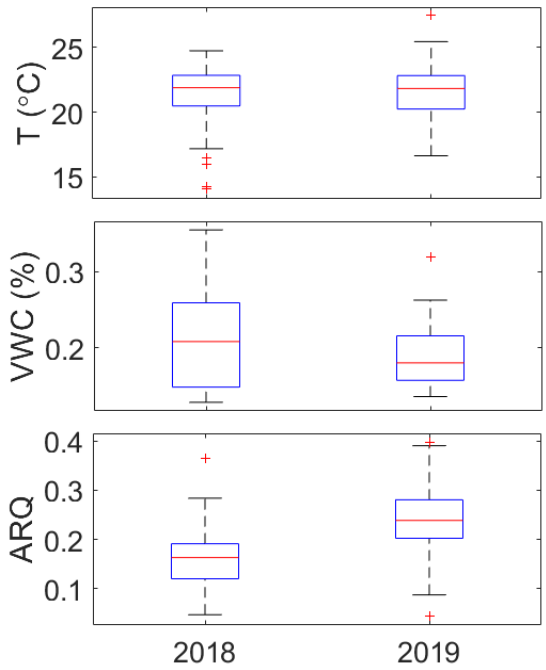

Figure 14: Box plot comparison between Victory Garden West plot variability of soil temperature, VWC, and ARQ in 2018 and 2019. The median is shown with the red line, upper and lower quartiles outlined in blue, and outliers shown as red +.

4.1.4 Green Roof Field Data Results

The green roof on Engineering Hall in 2019 (June 13 – October 17) had consistently higher O_2 concentrations and lower CO_2 concentrations as compared to the other sites (see section 4.1.1, 4.1.2, 4.1.3, and 4.1.5). The green roof soil O_2 concentration varied between 17% and 21% consistently fluctuating on a diurnal timescale (Figure 15a). The CO_2 varied between 251 and 3,932 ppm also fluctuating on a diurnal timescale (Figure 15b). CO_2 was typically low when the soil was drying. The soil moisture varied in response to precipitation events between 5% and 52% VWC (Figure 15c). There were two noticeably drier periods in which the lack of precipitation resulted in a decrease in soil moisture from the middle of July into the beginning of August (Figure 15c). Soil

temperature throughout the summer months remained around 20°C or above and then in October began to decrease (Figure 15d).

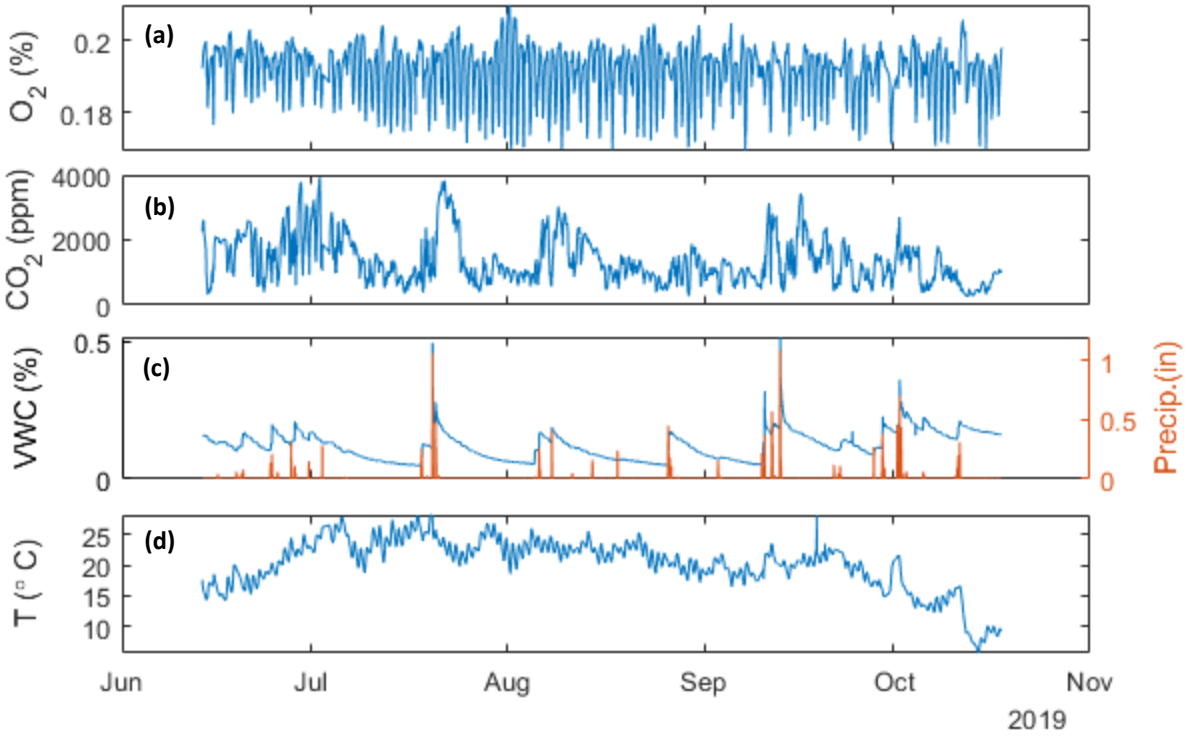

Figure 15. Timeseries of O_2 (a), CO_2 (b), VWC and precipitation (c) and soil temperature (d) at 15 cm deep in the green roof soil during June 13 – October 17, 2019.

For the green roof, O_2 was not significantly explained by either soil moisture or soil temperature. Linear regression analysis of the O_2 and temperature relationship resulted in an r^2 of 1% that was not significant ($p>0.05$, Figure 16a). Likewise, the linear regression analysis of the O_2 and VWC relationship resulted in an r^2 of 2% that was not significant ($p>0.05$, Figure 16b). Since the O_2 concentrations remained near atmospheric levels of 20.95%, ARQ variability may have been controlled by soil CO_2 concentrations. Therefore, this analysis considered the linear relationships of CO_2 concentration with the soil conditions. CO_2 concentrations increased with both soil temperature and VWC. Linear regression suggested CO_2 relationship to soil temperature was not highly linear

with a reported r^2 of 4%, although the relationship was significant ($p<0.05$; Figure 16c). Meanwhile, linear regression showed VWC explained 10% of CO_2 variability and the relationship was significant ($p<0.05$; Figure 16d).

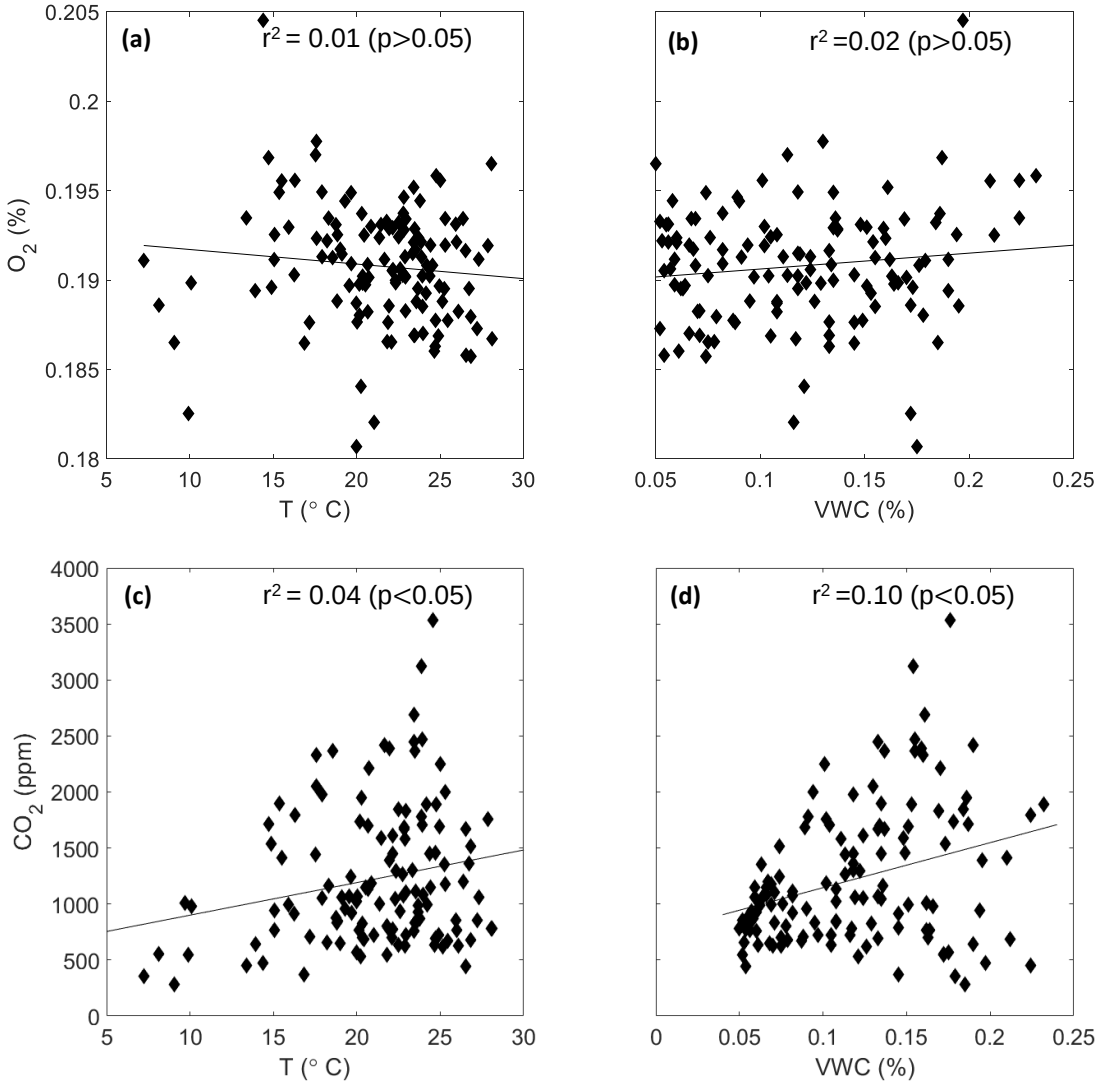

Figure 16. Correlation between daily O_2 and soil temperature (a) and soil moisture (b) and between daily CO_2 and soil temperature (c) and soil moisture (d) at the green roof plot for June 13 through October 17, 2019. The black line corresponds to the linear regression line.

The ARQ variability was explained by VWC but not by temperature at the green roof in 2019. ARQ did not respond to temperature with a linear regression r^2 of 1% that

was not significant ($p>0.05$, Figure 17a). Meanwhile, ARQ increased with VWC, where VWC explained 14% of ARQ variability and the relationship was significant ($p<0.05$, Figure 17b). The green roof was unique in the sense that daily ARQ stayed relatively low (ARQ<0.13) throughout the four months.

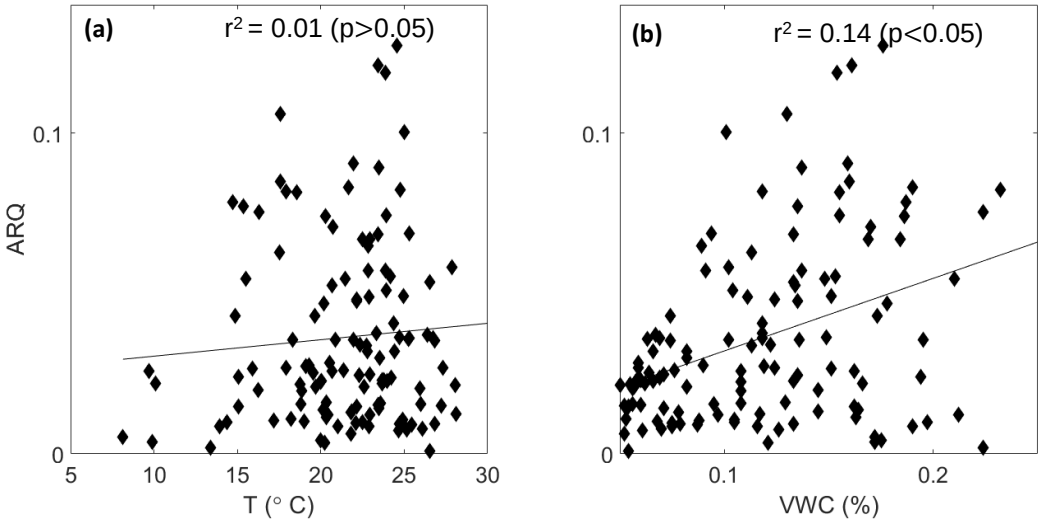

Figure 17. Correlation between daily ARQ and soil temperature (a) and soil moisture (b) at the green roof for June 13 through October 17, 2019. The black line corresponds to the linear regression line.

4.1.5 MMSD Wetland Field Data Results

In 2019 (May 14 – October 16), the soil temperature, O_2, and CO_2 all fluctuated on a daily scale and soil VWC fluctuated in response to precipitation events at the MMSD wetland site. The wetland soil O_2 concentration varied between 12 and 20% (Figure 18a) and CO_2 varied between 1,620 and 6,180 ppm (Figure 18b). The soil VWC was highly variable (14 – 44%) and did not show obvious seasonal transitions but rather fluctuated consistently in response to precipitation events (Figure 18c). The soil temperature remained between 19 and 13 °C for the majority of the collection period. An

increase in temperature occurred from May 14 to mid-July then decreased in October (Figure 18d).

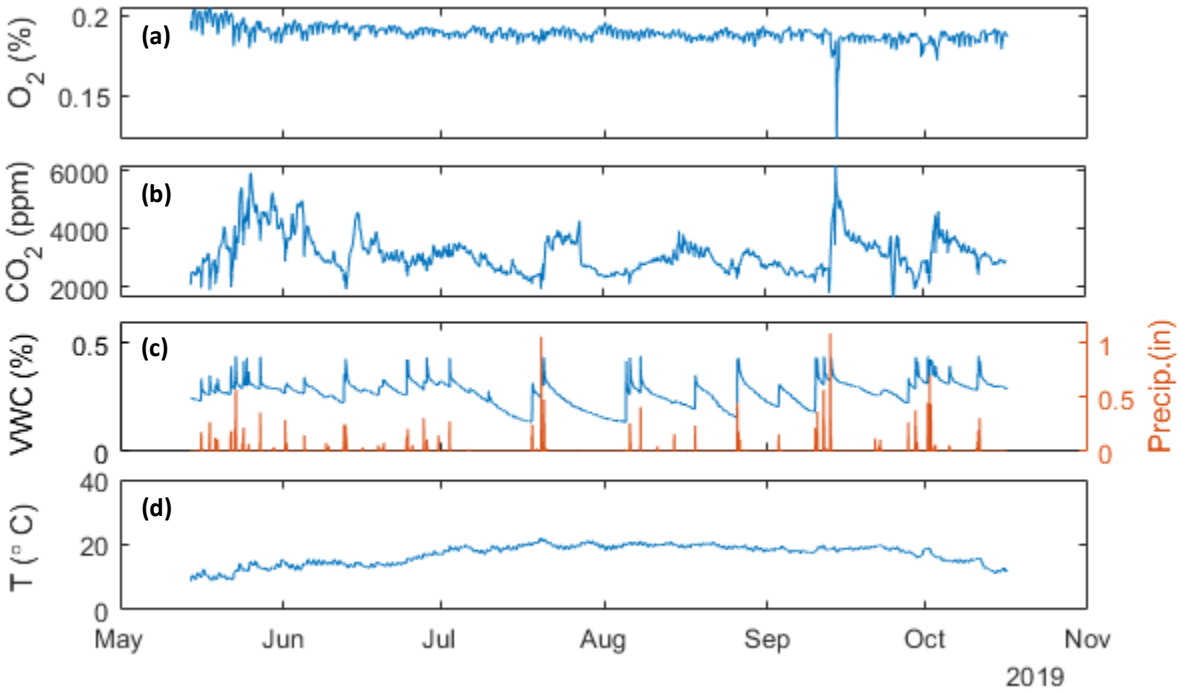

Figure 18. Timeseries of O_2 (a), CO_2 (b), VWC and precipitation (c) and soil temperature (d) at 15 cm deep in the MMSD wetland during May 14 to October 16, 2019.

Soil O_2 concentrations decreased with temperature. Linear regressions showed soil temperature explained 29% of the O_2 variability and the relationship was significant ($p<0.05$, Figure 19a), while O_2 did not respond to VWC with a linear regression r^2 of 2% that was not significant ($p>0.05$, Figure 19b).

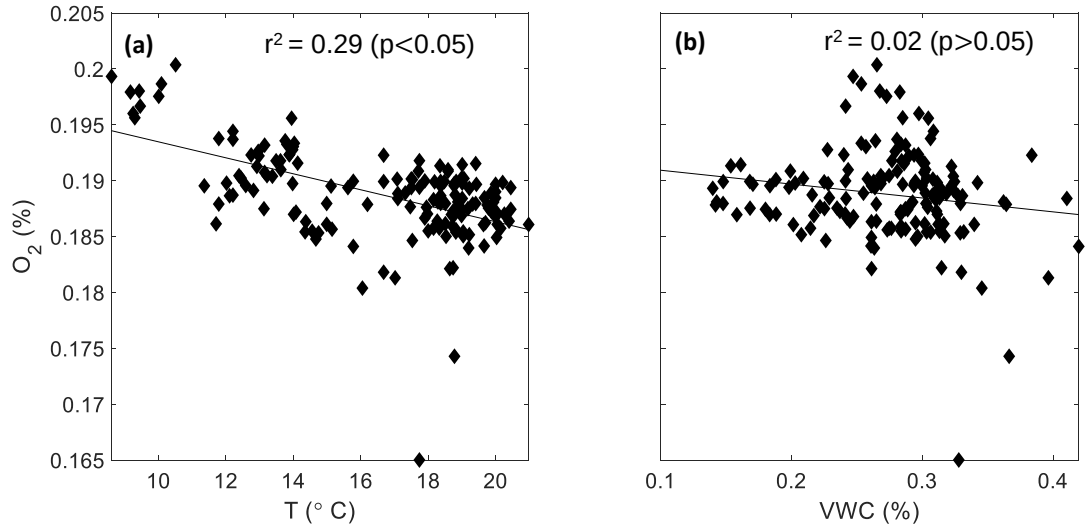

Figure 19. Correlation between daily O_2 and soil temperature (a) and soil moisture (b) at the MMSD wetland for May 14 through October 16, 2019. The black line corresponds to the linear regression line.

The ARQ variability was explained more by soil temperature than VWC at the MMSD wetland. ARQ decreased with soil temperature. Linear regressions showed soil temperature explained 33% of the variability of ARQ values and the relationship was significant ($p<0.05$, Figure 20a). On the other hand, ARQ did not respond to VWC with a linear regression r^2 of 3% that was not significant ($p>0.05$, Figure 20b). ARQ displayed large variability at a VWC of around 30%.

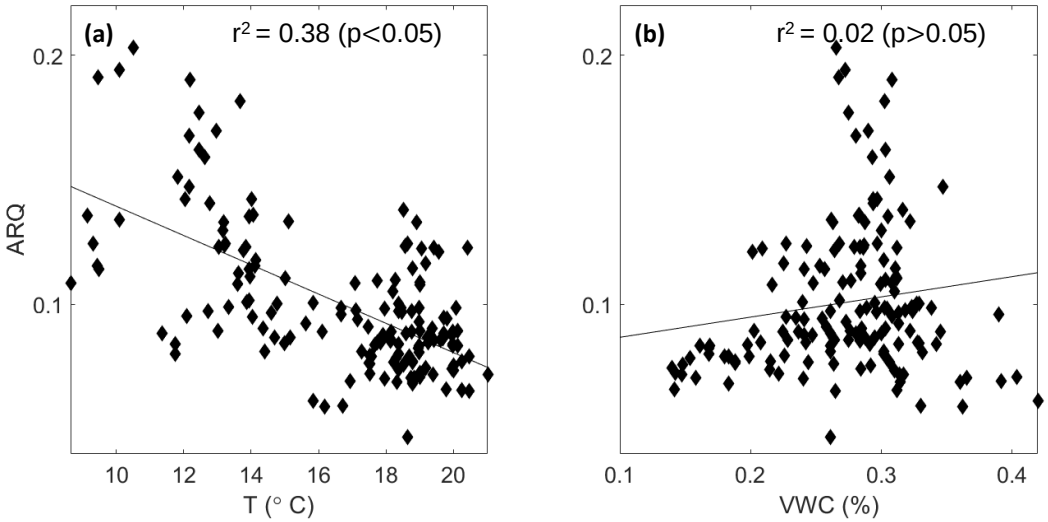

Figure 20. Correlation between daily O_2 and soil temperature (a) and soil moisture (b) at the MMSD wetland for May 14 through October 16, 2019. The black line corresponds to the linear regression line.

4.1.6 Three Bridges Park Wetland Field Data Results

In the Three Bridges Park wetland lowland plot in 2019 (May 18 – October 16) the soil temperature, O_2, and CO_2 all fluctuated on a daily scale and soil VWC fluctuated in response to precipitation events. The O_2 concentration varied between nearly 0 and 20% (Figure 21a) and CO_2 concentration ranged between 10,392 and >40,000 ppm (Figure 21b). At several instances the CO_2 concentration increased above the probe calibration limit of 40,000 ppm. The lowland plot at this site was the only plot where intermittent standing water was observed where the sensors were deployed. VWC levels remained high, between 35% and 45% throughout the collection period (Figure 21c). The soil temperature gradually increased from mid-May to mid-July then decreased from August to the end of the collection period in October (Figure 21d).

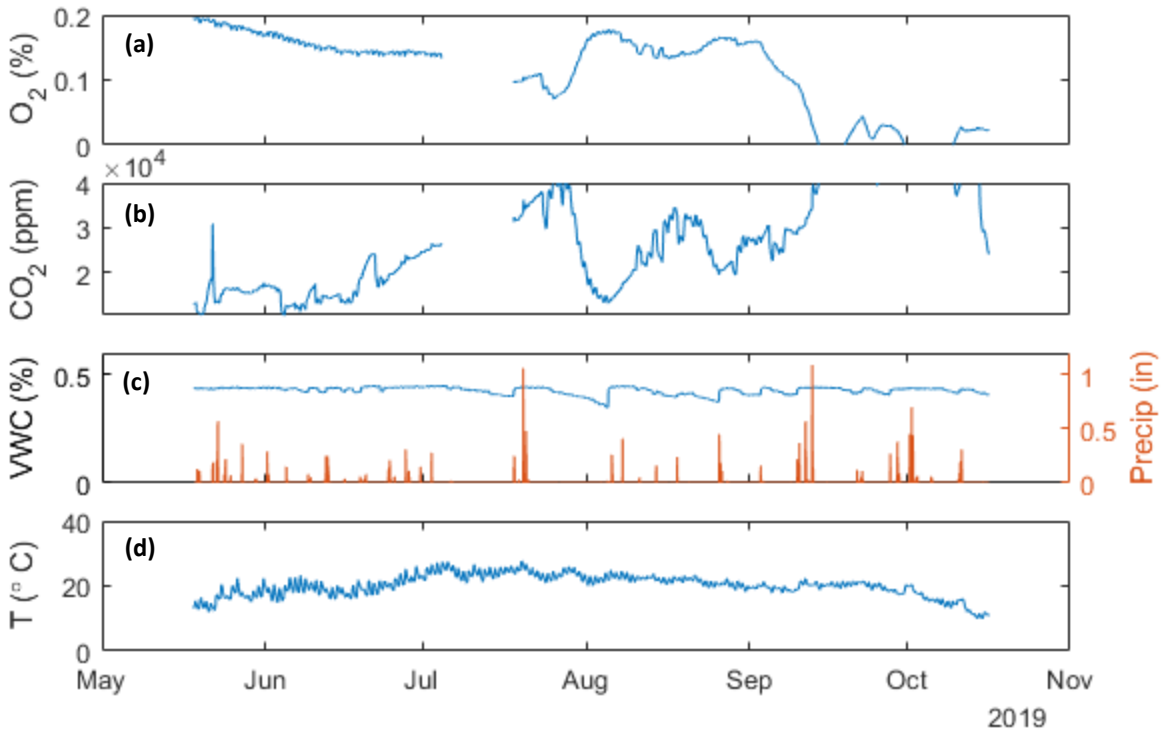

Figure 21. Timeseries of O_2 (a), CO_2 (b), VWC and precipitation (c), and soil temperature (d) at 15 cm deep in the lowland plot at Three Bridges Park wetland during May 18 to October 16, 2019. There are 2 gaps in the data. In July, 15 days were removed due to abnormality in the data. In September and October, some O_2 values read negative and some CO_2 values exceeded the probe calibration limit of 40,000 ppm.

At the Three Bridges Park wetland upland plot, the collection period ended September 30, 2019 due to a CO_2 sensor malfunction. The O_2 concentration varied between 11% and 20%, but remained above 18% starting July 4 until the end of September (Figure 22a). The CO_2 concentration ran above detection range (40,000 ppm) at the end of June into the beginning of July (Figure 22b). Then CO_2 concentration remained below 20,000 ppm from August through September (Figure 22b). Additionally, the VWC varied between the 14% and 45%, fluctuating with precipitation events (Figure 22c). The soil temperature was lowest in mid-May and then increased to 29 °C on July 4 (Figure 22d). From mid-July until the end of September the average soil temperature

gradually dropped to around 17 °C, all while the temperature fluctuated on a diurnal time scale (Figure 22d).

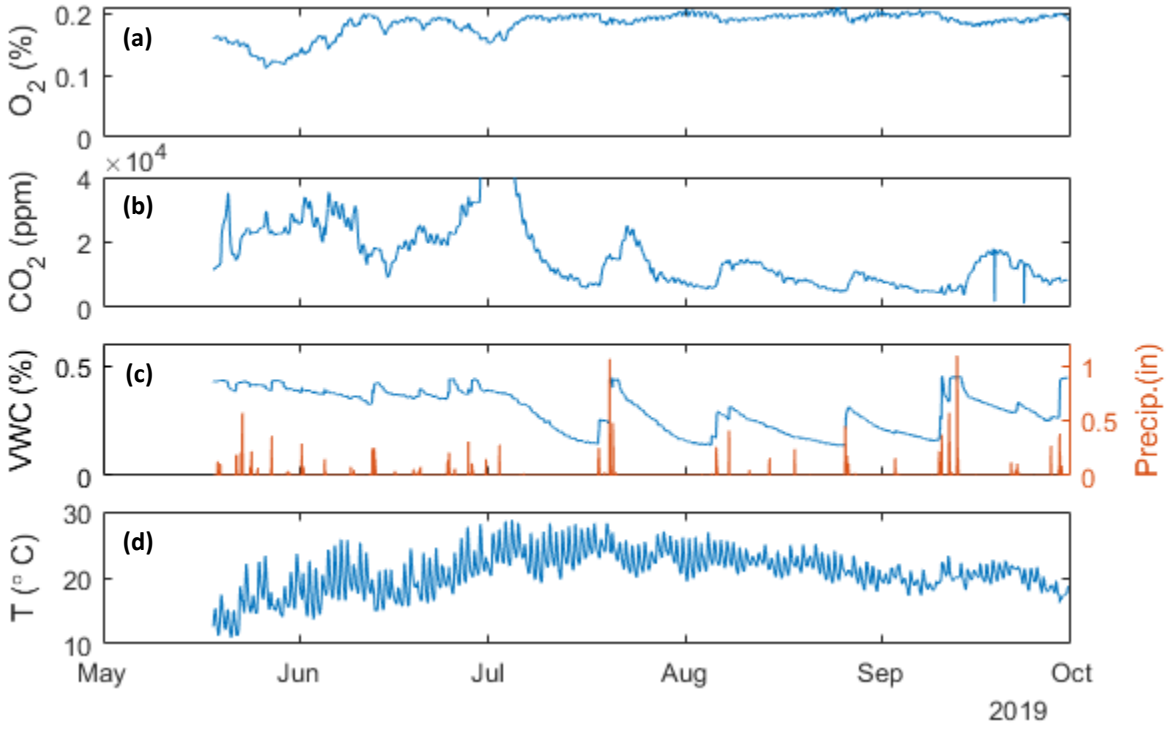

Figure 22. Timeseries of O_2 (a), CO_2 (b), VWC and precipitation (c) and soil temperature (d) at 15 cm deep in the upland plot at Three Bridges Park wetland during May 18 to September 30, 2019. The gap in CO_2 data in July occurred because soil CO_2 concentrations exceeded the probe calibration limit of 40,000 ppm.

Soil O_2 concentrations in the Three Bridges Park wetland upland plot increased with soil temperature. Linear regression showed the soil temperature explained 25% of the ARQ variability and the relationship was significant ($p<0.05$, Figure 23a). The daily O_2 decreased with soil moisture in the upland plot. Linear regression showed the VWC explained 45% of the O_2 variability and the relationship was significant ($p<0.05$, Figure 23b). The daily O_2 concentrations in the lowland plot did not respond to soil temperature. Linear regression analysis resulted in an r^2 of 1% that was not significant ($p>0.05$, Figure 23c). The daily O_2 also did not respond to VWC in the lowland plot, in which the linear

regression analysis resulted in an r^2 of 0.2% that was not significant ($p>0.05$, Figure 23d). The variability of O_2 increased at a VWC of around 40% at both locations (Figure 23b and d).

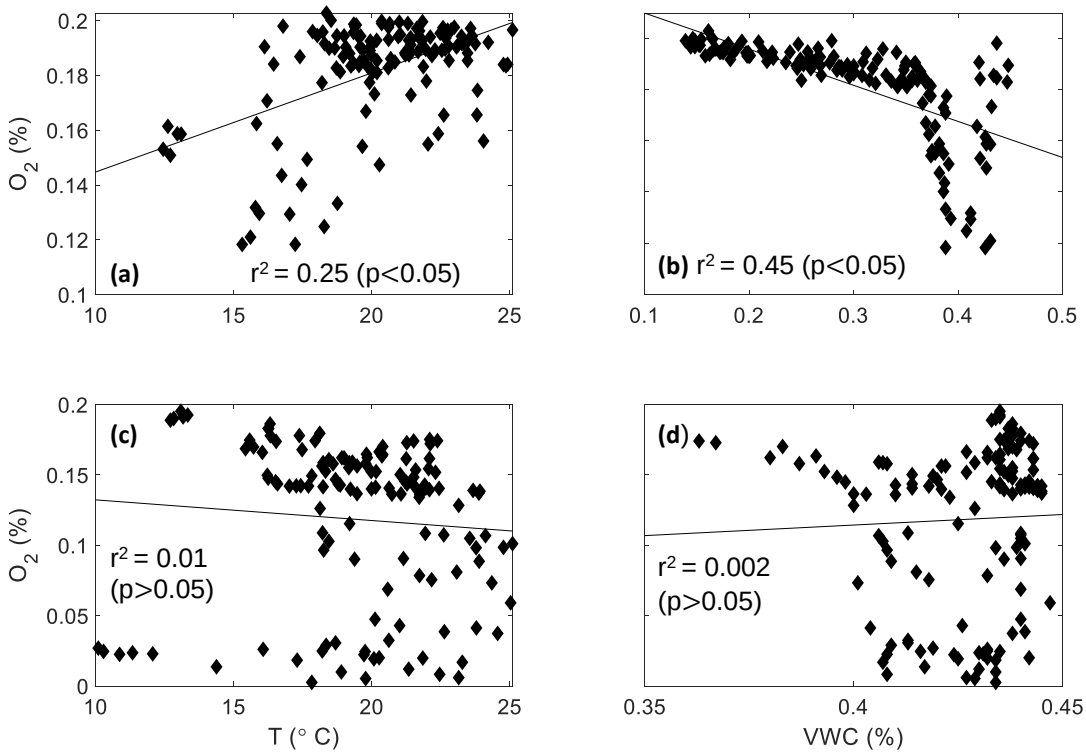

Figure 23. Correlation between daily O_2 and soil temperature (a) and VWC (b) at the wetland upland plot for May 18 through September 30, 2019 and correlation between daily O_2 and soil temperature (c) and VWC (d) at the wetland lowland plot for May 18 through October 16, 2019. The black line corresponds to the linear regression line.

The ARQ variability was not explained by either soil temperature or VWC in both the lowland and upland plots. Linear regression suggested the ARQ response to VWC was not linear in the upland plot with a reported r^2 of 8%, although the relationship was significant ($p<0.05$, Figure 24a). Additionally, ARQ did not respond to soil temperature in the upland plot with a linear regression r^2 of 1% that was not significant ($p>0.05$, Figure 24b). Also, linear regression of the lowland plot data suggested ARQ was not

strongly linearly related to soil temperature with a reported r^2 of 7%, although the relationship was significant ($p<0.05$, Figure 24c). ARQ did not respond to VWC with a linear regression r^2 of 0.01% that was not significant ($p>0.05$, Figure 24d). Like O_2, the ARQ was more variable in higher VWC conditions in both locations (Figure 24b and d).

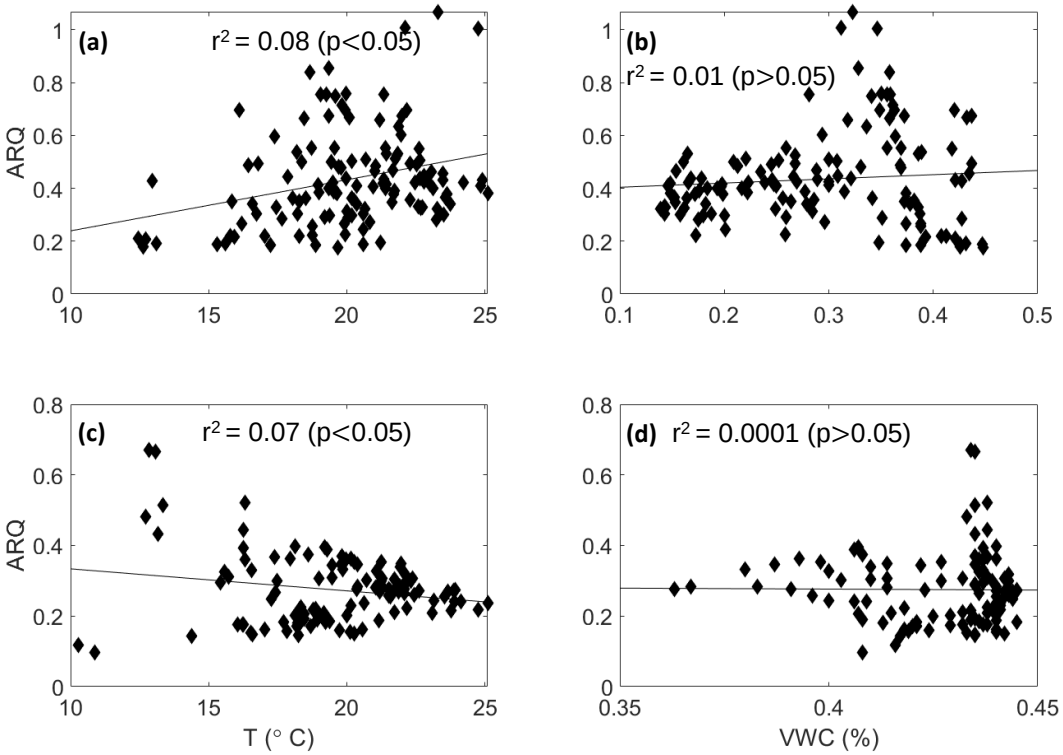

Figure 24. Correlation between daily ARQ and soil temperature (a) and soil moisture (b) at the wetland upland plot for May 18 through September 30, 2019 and correlation between daily ARQ and soil temperature (c) and soil moisture (d) at the wetland lowland plot for May 18 through October 16, 2019. The black line corresponds to the linear regression line.

4.1.7 Cross Site Results

Overall, the VWC range in six of the seven sets of data were similar (Figure 25a). The wettest site was the Three Bridges Park wetland lowland plot in which the VWC typically stayed above 40%. The driest site was the green roof where the median VWC

was 12%. The other sites including the Victory Garden plots, MMSD wetland, and Three Bridges Park wetland upland plot had VWC medians between 20% and 40%.

Among the seven sets of data, the highest ARQ values were observed at the upland plot at Three Bridges Park wetland (Figure 25b). This site was also the most variable with ARQ readings ranging between 0.17 and 1.07. All Victory Garden data and the lowland plot of the Three Bridges Park wetland showed similar ARQ medians. The upland plot of the Three Bridges Park wetland, ARQ values were considerably higher than all other sites with a median of 0.41 over the five months. The wetland at MMSD had an ARQ median (0.09) below the Victory Garden (medians of 0.16, 0.14, and 0.18 in 2018, West plot, and East plot, respectively) and Three Bridges Park wetland lowland plot (median of 0.27). However, the MMSD ARQ median was above the green roof ARQ median of 0.03.

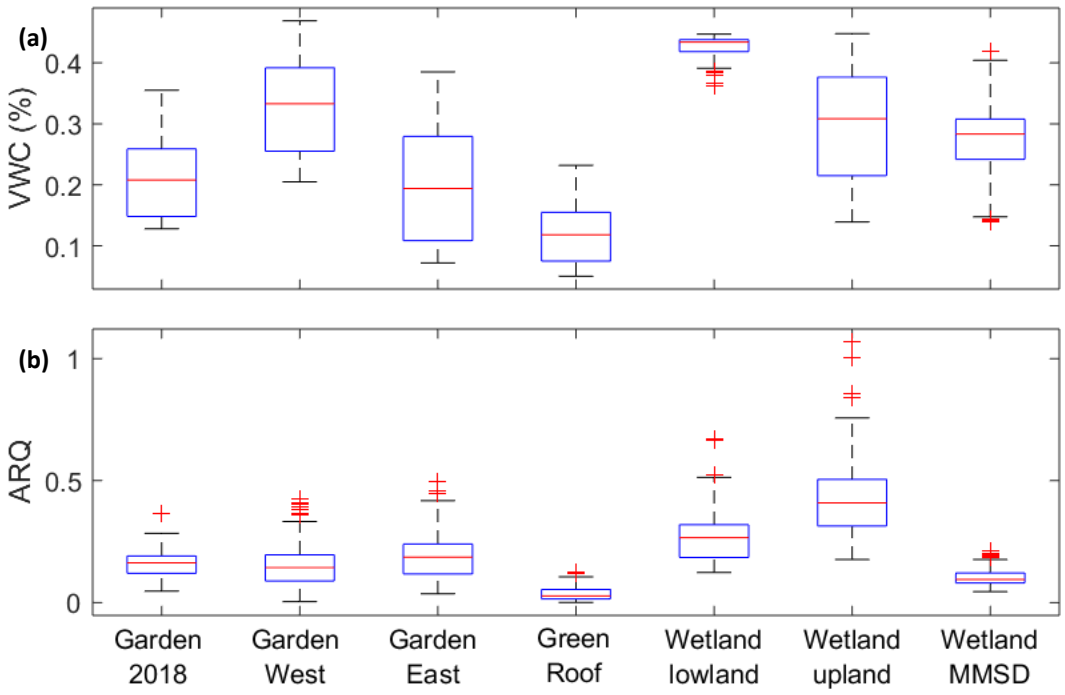

Figure 25. Box and whisker plot of VWC (a) and ARQ (b). The median is shown with the red line, upper and lower quartiles outlined in blue, and outliers shown as red +.

Three sites had a statistically significant relationship between ARQ and VWC, all of which displayed a positive linear relationship (Figure 26a). The steepest positive slope of ARQ against VWC was observed at the Victory Garden West plot (2018-yellow line, 2019-orange line, Figure 26a). It should be noted that this ARQ-VWC relationship had a 20% steeper positive slope in 2018 than in 2019. The relationship with the second steepest slope was at the green roof between ARQ and VWC (purple line, Figure 26a). In the other sites, ARQ increased with VWC but had more ARQ variability in wetter conditions (Figure 26a). Linear regression analysis results between CO_2 and VWC showed CO_2 increased with VWC at all the sites ARQ significantly responded to VWC (Table 4). Additionally, Victory Garden West in both 2018 and 2019 had O_2 decrease with VWC and the relationship was significant ($p<0.05$, Table 4).

The relationship between ARQ and soil temperature was less consistent across sites. Three sites displayed a negative linear relationship and two sites displayed a positive linear relationship (Figure 26b). The three sites with a negative relationship between ARQ and temperature all had similar slopes; meanwhile, the two sites that increased with soil temperature did not. Table 5 summarizes the linear regression analysis results between temperature and ARQ, O_2, and CO_2 at all sites. The sites had varying strength and significance in O_2 or CO_2 response to temperature, similar to the ARQ response to temperature (Table 5).

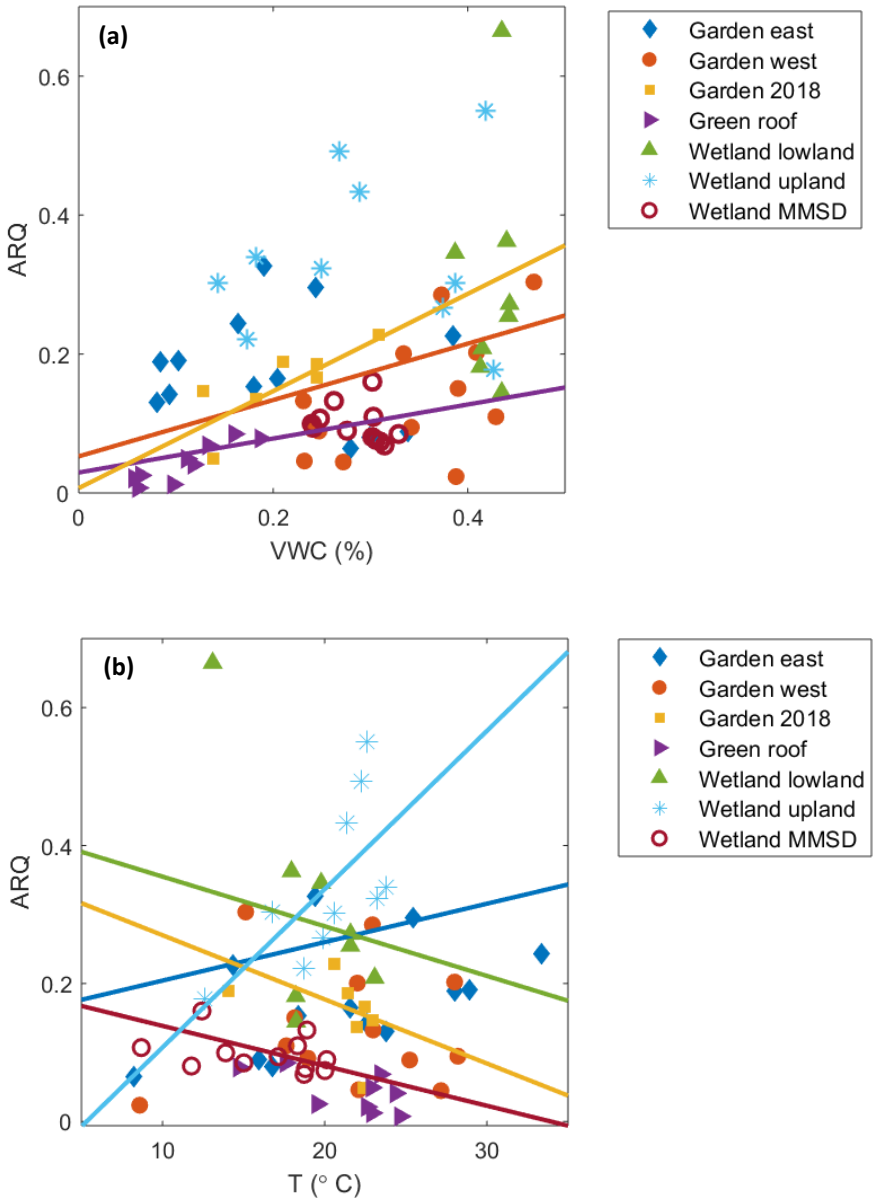

Figure 26: Correlation between daily sampled ARQ and soil moisture (a) and soil temperature (b) at all sites. Significant linear regressions with $p<0.05$ have trendlines plotted in the color corresponding to the site. Between ARQ and VWC, Victory Garden West, Victory Garden 2018 and green roof had significant linear regressions. Between ARQ and temperature, Victory Garden East, Victory Garden 2018, Three Bridges Park wetland lowland, Three Bridges Park wetland upland, and MMSD wetland had significant linear regressions.

***Table 4**: Summary table of ARQ, O_2, and CO_2 linear relationships with soil moisture (VWC) at each site. The significant probability values of less than 0.05 are identified with the **bolded values**. The slopes of all linear relationships were identified as either positive (+) or negative (-).*

	ARQ – VWC			***O_2 – VWC***			***CO_2 – VWC***		
Site	***r^2***	***p***	***+/-***	***r^2***	***p***	***+/-***	***r^2***	***p***	***+/-***
Wetland MMSD	0.022	0.081	+	0.023	0.21	-	**0.079**	5.5e-4	-
Green roof	**0.14**	2.2e-5	+	0.016	0.17	+	**0.10**	4.2e-4	+
Victory Garden East	0.0010	0.69	-	0.0018	0.56	+	0.0015	0.58	-
Victory Garden West	**0.11**	1.4e-6	+	**0.083**	4.0e-5	-	**0.14**	4.8e-8	+
Victory Garden 2018	**0.41**	2.5e-11	+	**0.51**	1.4e-14	-	**0.58**	2.3e-17	+
Wetland upland	0.0070	0.35	+	**0.45**	7.1e-19	-	**0.52**	2.2e-22	+
Wetland lowland	~0	0.95	-	0.0020	0.61	+	0.014	0.19	-

***Table 5**: Summary table of ARQ, O_2, and CO_2 linear relationships with soil temperature (T) at each site. The significant probability values of less than 0.05 are identified with the **bolded values**. The slopes of the linear relationships were identified as either positive (+) or negative (-).*

	ARQ – T			***O_2 – T***			***CO_2 – T***		
Site	***r^2***	***p***	***+/-***	***r^2***	***p***	***+/-***	***r^2***	***p***	***+/-***
Wetland MMSD	**0.38**	4.7e-15	-	**0.29**	2.0e-12	-	**0.042**	0.014	+
Green roof	0.0053	0.42	+	0.012	0.25	-	**0.042**	0.023	+
Victory Garden East	**0.075**	1.0e-4	+	**0.045**	0.0030	-	**0.20**	3.3e-11	+
Victory Garden West	0.0010	0.73	+	**0.27**	8.7e-15	-	**0.041**	0.0041	+
Victory Garden 2018	**0.065**	0.018	-	**0.082**	0.0075	+	**0.061**	0.021	-
Wetland upland	**0.082**	9.8e-4	+	**0.25**	8.6e-10	+	**0.073**	0.0019	-
Wetland lowland	**0.035**	0.050	-	0.0068	0.34	-	**0.35**	2.2e-11	+

4.1.8 Seasonality Analysis

To analyze the seasonal variability of the data, linear regressions were calculated on the data over several three-month periods, each shifted by one week throughout the collection period. The results of this analysis showed each site responded differently to temperature (Figure 27). The Victory Garden plots both had positive ARQ-temperature relationships in spring seasons starting between March 29 and April 19 and then had negative ARQ responses to temperature until June 21 for the Victory Garden East plot and until July 26 for the Victory Garden West plot. The wetland plots all experienced

different relationships between ARQ and temperature throughout the year. The Three Bridges Park wetland upland plot had mostly positive regressions except for two periods June 1 – August 1 and June 8 – August 8. Meanwhile, the Three Bridges Park wetland lowland plot had a positive relationship between ARQ and temperature during periods of May 25 to July 15 and July 13 to August 3, 2019. The MMSD wetland gradually displayed positive linear regressions in the later part of the collection period (Figure 27).

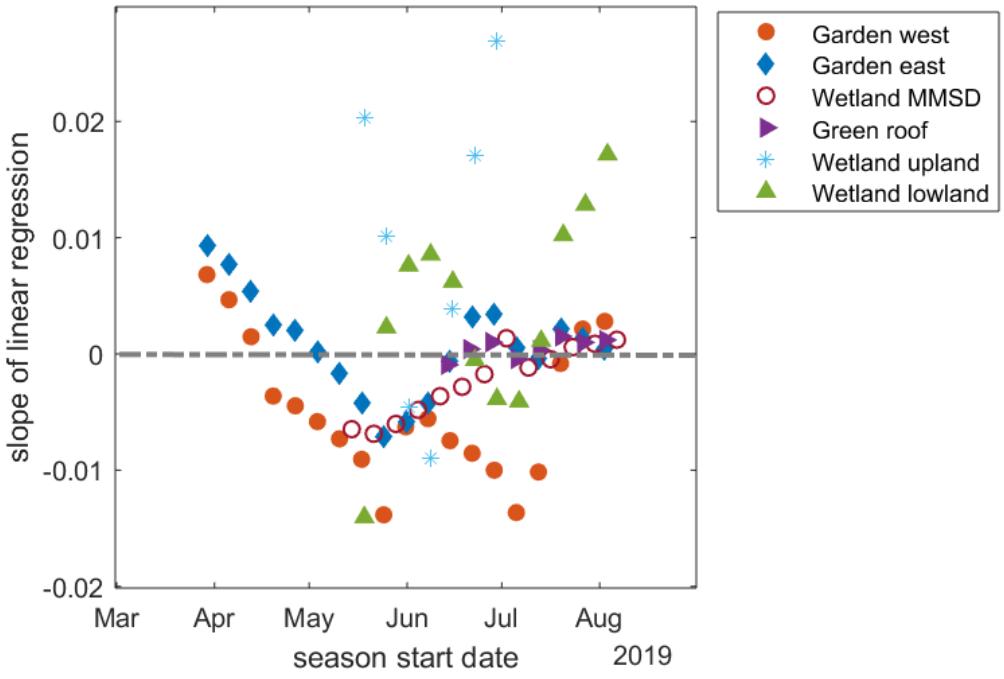

Figure 27: Slopes of linear regressions between ARQ and soil temperature at all sites for a three-month moving window. Each point represents the slope of a linear regression on three-months of data and the x-coordinates of the points identify the start of each period.

The seasonal analysis showed that in general the sites showed a positive relationship between ARQ and VWC (Figure 28). In contrast, the Three Bridges Park wetland lowland plot had a consistently negative ARQ and VWC relationship, with one exception period in May. The Victory Garden East plot showed negative relationships between ARQ and VWC in the early seasons starting in April. For all other periods, the

Victory Garden East plot showed positive relationships between ARQ and VWC. The Victory Garden West plot, MMSD wetland, green roof, and Three Bridges Park wetland upland plot all showed positive relationships between ARQ and VWC with slopes that decreased toward the end of the year.

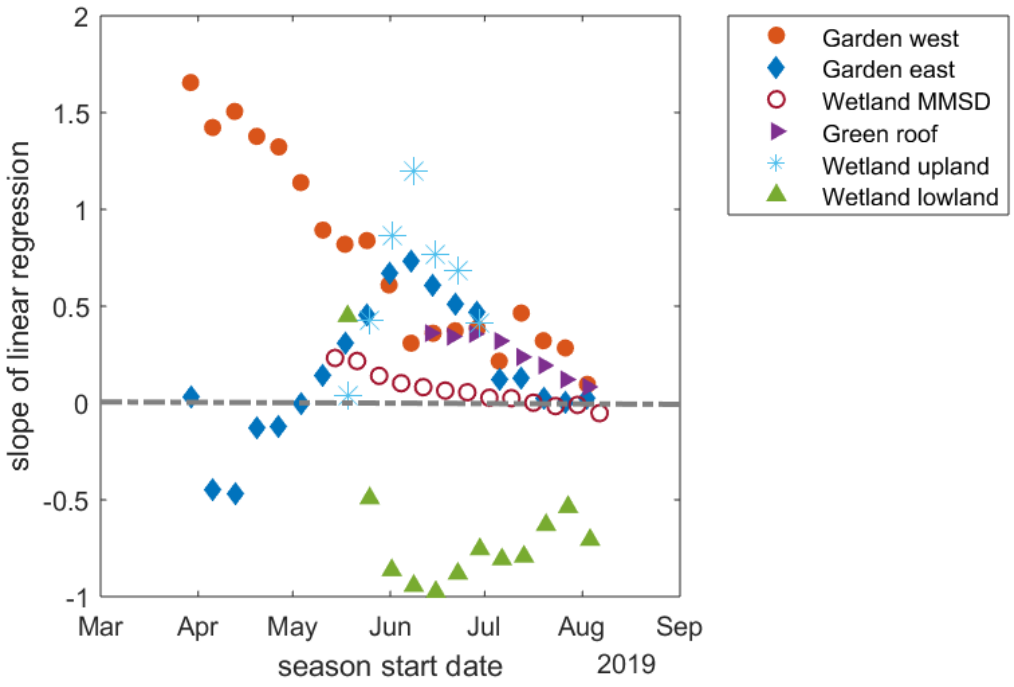

Figure 28: Seasonal regressions between ARQ and VWC at all sites. Each point represents the slope of a linear regression on three-months of data and the x-coordinates of the points identify the start of the three-month period.

4.2 CO_2-O_2 Phase Space Analysis

The CO_2-O_2 phase space analysis showed that across most sites the CO_2 concentrations were less than what was predicted by Equation (5) with the assumption that all biogeochemical activity was due to aerobic biological respiration (i.e., $\alpha = 1$) (Figure 29). One exception was the CO_2-O_2 points at the Three Bridges Park wetland upland plot in which the data on 33 days were located between the relationships for

aerobic biological respiration ($\alpha = 1$) and methane oxidation ($\alpha = 0.5$). The Three Bridges Park wetland upland plot had high O_2 concentrations between 16.6% and 19.6% when CO_2 concentrations were high (2 - 4%) (green dots, Figure 29). The Three Bridges Park wetland lowland plot showed similar CO_2 concentrations, however, at this site the O_2 was as low as 0.6% (purple dots, Figure 29). This resulted in the Three Bridges Park wetland lowland plot CO_2-O_2 relationships being much lower than the theoretical predictions for methane oxidation. All other locations had high O_2 percentages but showed less CO_2 produced than predicted by either biological respiration or methane oxidation.

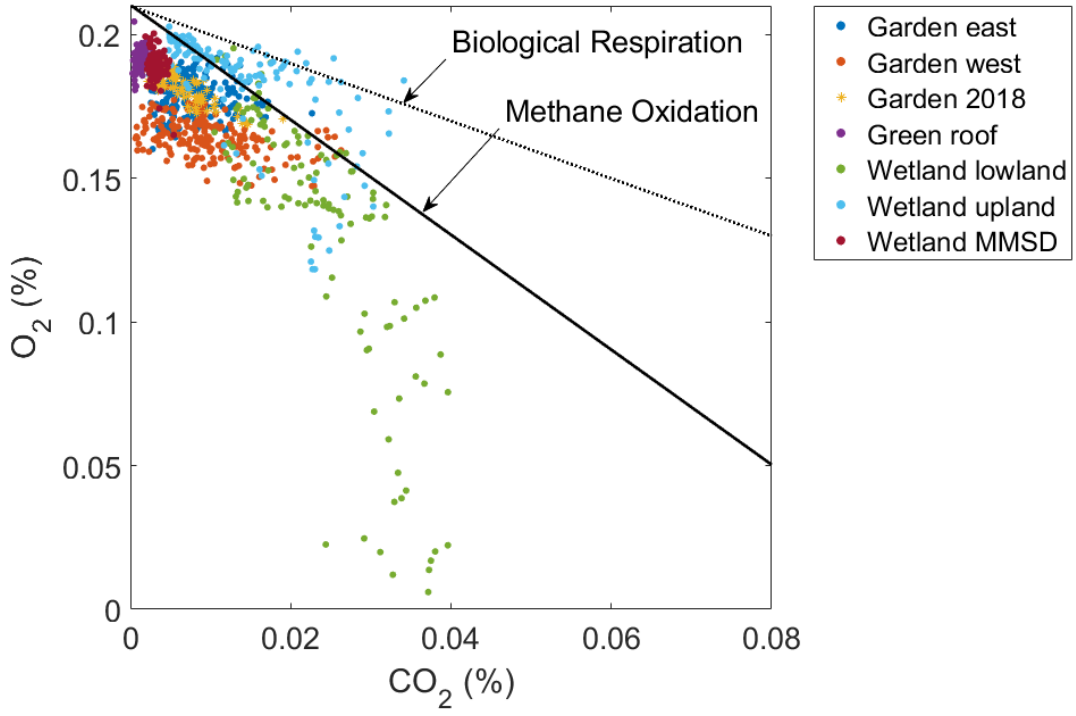

Figure 29. Soil O_2 and CO_2 concentration data for all sites. Theoretical predicted processes of biological respiration and methane oxidation are shown with a dotted and solid line, respectively. These reference processes show the predicted relationship between O_2 and CO_2based on their stoichiometric equations (Equation 5).

4.3 Model Results

In simulation (1), ARQ slightly increased with VWC (Figure 30, solid line). Since α was set to 1, it was expected that the modelled ARQ would be equal to 1. Although this simulation resulted in ARQ changing with VWC, ARQ stayed near 1 and increased by only 4% across the range of VWC. When VWC was variable but α was held constant, the ARQ values typically followed the previous simulation results (Figure 30, open circles). The ARQ values were more variable in comparison to the steady-state simulation, especially with a VWC of 30% or greater. Most ARQ values fell around the assumed value of α =1, with a mean of 0.98 and standard deviation of 0.020. When VWC was

high, the ARQ values increased. This increase in ARQ at higher VWC was attributed to the physical transport of gases under saturated conditions.

Lastly, in the simulation with both α and VWC as variable, ARQ increased with VWC with a greater slope than the other two simulations (Figure 30, triangles). For this simulation, α was variable between the values of 0 and 1 by assuming α was dependent on VWC. When α was variable, ARQ varied between 0.3 and 0.9 which was more representative of ARQ values seen in the field.

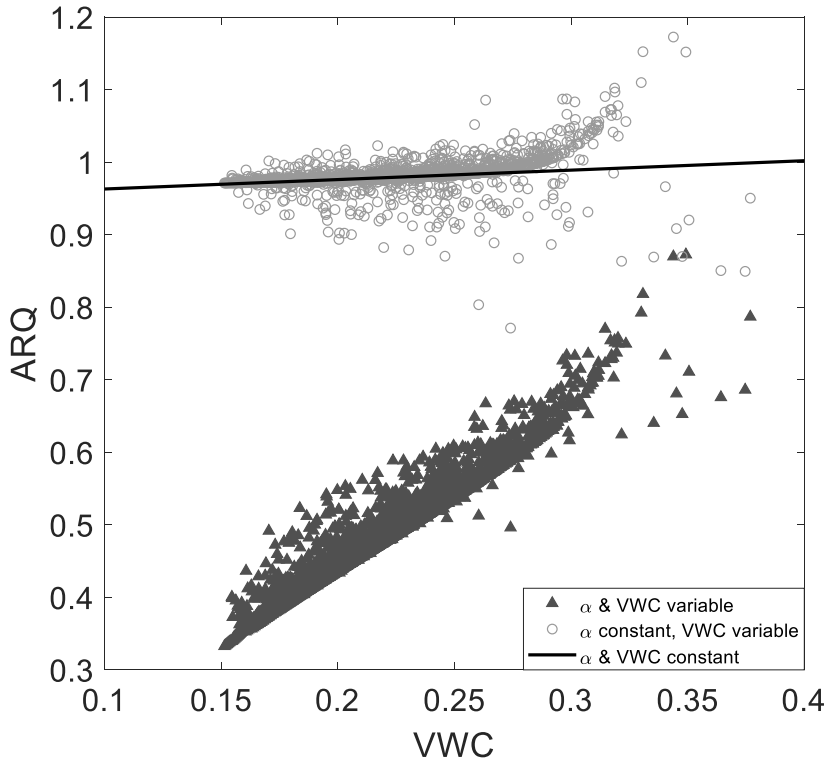

Figure 30: ARQ versus VWC relationships obtained from the three model simulations, The simulations were (1) α and VWC constant (solid black line), (2) α constant and VWC variable (opened circles), and (3) α linearly increased with VWC and VWC variable (filled triangles).

4.4 Summary of Results

Between the field data and model simulations, this research found several results regarding biogeochemistry in urban GSI soils. Based on the research objectives three important conclusions have been made.

1. Linear regressions of three-month periods and of the entire data showed ARQ generally increased with soil moisture. The one exception consistently being Three Bridges Park wetland lowland plot where ARQ responded negatively to VWC. At this location, the only site to experience intermittent standing water, either low biological activity occurred or a process like CO_2 dissolution may have been the main driver of gas concentrations. The results from the other sites suggest biogeochemical processes with high ARQ respond positively to increased soil moisture.
2. Linear regressions of the three-month periods of data demonstrated the sites to have "peak" periods during which the ARQ positively responded to soil temperature. The linear regressions on the entire data showed significant positive ARQ response to temperature at Three Bridges Park wetland upland plot and Victory Garden East plot, and significant negative relationships at Victory Garden West 2018, MMSD wetland, and Three Bridges Park wetland lowland. These relationships may be skewed because each site experienced a specific peak period that may result in generally positive or negative responses over the collection period of this study.

3. Model results suggest that the observed variability in ARQ was likely driven by biogeochemical process response to soil moisture, as opposed to the physical response of diffusivity to soil moisture. When only physical processes varied with soil moisture, ARQ remained near the control simulation ARQ results. When biogeochemical and physical processes varied with soil moisture, the ARQ values deviated from the control simulation and increased with soil moisture, thus supporting the assumption that ARQ variability is driven by biogeochemical responses to soil moisture.

5. DISCUSSION

5.1 Spatial and Temporal ARQ Variability

Most notably, the positive response of ARQ to soil moisture was similar across most sites. Soil microorganism activity has been noted to respond quickly to soil moisture after being dormant during low moisture conditions (Liu et al., 2019). The positive microbial response to soil moisture could explain the repeatable positive relationship between ARQ and VWC during the growing season. If microbial activity responds to an increase in VWC, both anaerobic and aerobic microbial activity would increase the ARQ values. However, seasonal microbial and plant dormancy may result in a non-responsive or negative relationship, such as in April in the Victory Garden East plot, which showed ARQ had a negative response to VWC. The empirical model created by Moyano et al. (2012) found that the respiration response to soil moisture was positive in clay and silt soils as well as in the presence of organic carbon. The GSI soils at these research sites may also consist of finer textured soils or high organic carbon content, which may partially explain the positive response between ARQ and VWC at the sites.

When soil moisture values were above 30%, the ARQ values were more variable in both the field data and modelled data. Others have suggested that the increase in soil moisture activates respiration (Hodges et al., 2019; Riveros-Iregui et al., 2007, 2011). At higher VWC conditions, seasonal hysteresis has been noted in which the early summer has higher respiration quotients than early spring months at the same VWC (Hicks Pries et al., 2019).

The regressions between ARQ and soil temperature over the entire collection time showed that the relationship was site-dependent. The reason why the relationships were different at the different sites was best explained with the season analysis. The relationship between soil temperature and respiration has been noted before (Lloyd & Taylor, 1994; Risk et al., 2002; Zhang et al., 2015), but generally as a positive relationship. The seasonal analysis between ARQ and soil temperature indicated that at each site, the relationship shifted between positive and negative depending on the season and site. The seasonal response can be interpreted as the dominant driver of the ARQ response to seasonal temperature shifts. Similar to the findings of this study, Hodges et al. (2019) also found that ARQ varied seasonally, with higher ARQ values in summer to late summer and lower values in early growing season. This study attributed the seasonal response of ARQ to temperature or soil moisture changes.

The O_2 relationship with soil moisture confirmed prior results. The results showed that O_2 decreased with VWC for all sites. Other studies have found a similar trend of VWC limiting O_2 (Liptzin et al., 2011; Silver et al., 1999). The only site to experience low O_2 concentrations was the lowland plot at Three Bridges Park. At all other locations, O_2 concentrations remained above 12%. These higher O_2 concentrations were similarly observed in the studies by Angert et al. (2015), Hicks Pries et al. (2019), and Sanchez-Canete et al. (2018) in soil depths of 30 cm or less. The high O_2 concentrations may indicate low O_2 consumption near the surface or the soils at these depths were similarly well-aerated.

Spatially, the ARQ values were lower than that predicted for aerobic metabolism at all sites except for the Three Bridges Park wetland upland plot. A spatial

biogeochemical study at the Susquehanna Shale Hills Critical Zone Observatory by Hodges et al. (2019) found that in growing seasons of 2015, 2016, and 2017, ARQ was typically less than 1. On the mid-slopes and ridgetops, ARQ increased above 1 (Hodges et al., 2019). The field results from this study found similar results, where the Three Bridges Park wetland lowland plot had consistently lower ARQ values, and the Three Bridges Park wetland upland plot had higher ARQ values.

When soils undergo drying and wetting, CO_2 has been noted to increase with wetting (Orchard & Cook, 1983). The increase in CO_2 and respiration due to the wetting of the soil may be better explained with the Birch Effect. The Birch Effect is explained as the spiked microbial activity in circumstances of intermittent wetting and drying conditions causing a large increase in CO_2 emissions (Moyano et al., 2013). The Birch Effect has also been noted to increase microbial biomass (Xiang et al., 2008). All the sites experienced intermittent wetting and drying conditions except the Three Bridges Park wetland lowland plot. Instead, the Three Bridges Park wetland lowland plot had consistently wet soils in which respiration did not respond to high VWC conditions. The lack of drying conditions could therefore help explain the low ARQ values at the Three Bridges Park wetland lowland plot. Additionally, at the Three Bridges Park wetland lowland plot, limited CO_2 diffusion from high moisture could result in the transfer from gas to soluble state, thus depleting CO_2 concentrations and lowering ARQ values (Angert et al., 2015; Olshansky et al., 2019).

The relationship between CO_2 and O_2 did not often result in an ARQ value of 0.76 predicted for aerobic metabolism. Instead, the sites had relatively low ARQ values, which would indicate aerobic respiration was not the only driver of gas concentrations. That is

not to say aerobic respiration did not occur; in fact, multiple processes may co-occur. The study by Hall et al. (2013) found aerobic and anaerobic metabolic processes to co-occur in their plots, suggesting there was spatial variation in soil moisture and O_2 availability within a soil profile. It was hypothesized that aerobic biological metabolism was occurring at all of the sites, but other processes occurred as well such as metal oxidation (e.g., Hicks Pries et al., 2019) or carbon dissolution (e.g. Sánchez-Cañete et al., 2018) causing a decrease in ARQ values from the predicted value of 0.76.

5.2 CO_2 – O_2 Phase Space Relationships

The CO_2-O_2 phase space analysis represents integrated biological and chemical activity in the field. In the phase space, CO_2 concentrations were consistently less than what would be expected from biological respiration. CO_2 concentrations may be lower due to processes like CO_2 dissolution (Elberling et al., 2011; Iiyama & Hasegawa, 2009; Ma et al., 2013; Romanak et al., 2012; Sánchez-Cañete et al., 2018). Three other potential drivers causing the slope between O_2 and CO_2 to be greater than -0.76 include silicate weathering, lignin mineralization, or abiotic/chemolithoautotrophic oxidation (Hodges et al., 2019).

5.3 Nutrient Uptake

Urban runoff entering GSI soils has been observed to contain nutrients that are harmful to receiving water ecosystems (Davis, 2007; Hunt et al., 2006; Kim et al., 2003; Li & Davis, 2014). ARQ data can give insight into the removal of those nutrients in the GSI system. Higher ARQ values suggest activity of anaerobic metabolism (Angert et al.,

2015). Predominance of anaerobic respiration may result in N removal via denitrification. The Three Bridges Park wetland upland plot had the highest ARQ values, thus suggesting this location had the highest N removal potential in comparison to the other GSI sites. On the contrary, lower ARQ values represent aerobic biogeochemical processes like root respiration and metal oxidation (Hodges et al., 2019). The presence of metals like iron has been shown to sequester P in stormwater systems (Okochi & McMartin, 2011). Metal oxidation would result in O_2 consumption without CO_2 production, which the data suggest may have occurred in the Three Bridges Park wetland lowland plot.

As mentioned in previous chapters, fluctuations between aerobic and anaerobic conditions have been found to increase denitrification (Reddy & Patrick, 1975), which can decrease the N in the GSI soils. Anaerobic metabolism can also drive the P and carbon concentrations, in addition to N concentrations (Burgin et al., 2011). Temporal fluctuations between aerobic and anaerobic metabolism may have occurred at these sites, where ARQ values varied significantly with soil moisture and reduced O_2 availability.

6. CONCLUSIONS

6.1 Key Findings

ARQ can be used to help distinguish what biogeochemical process is dominant in soils. ARQ values observed in this study suggested that chemical processes like metal oxidation and CO_2 dissolution occurred alongside biological respiration. Throughout the growing season the sites had plant growth but the corresponding ARQ values indicated that the root and microbial metabolism was not the only driver of gas concentrations. The ARQ is limited in directly identifying which biogeochemical process is occurring, however, it serves as a base index of the biogeochemical activity in soils.

From the field results of this study, in general, the ARQ increased in wetter soils. This relationship was seen spatially, temporally, and seasonally apart from the Three Bridges Park wetland lowland plot. Meanwhile, the relationship between soil temperature and ARQ was site-dependent. The linear regressions showed that some sites had a positive relationship between ARQ and soil temperature, while others had a negative relationship. The seasonality analysis gave more details regarding the relationship between soil temperature and ARQ relationship. The results showed that ARQ at different sites responded differently to temperature in different seasons. The seasonality analysis also confirmed that the relationship between ARQ and VWC was consistently positive across most seasons except for the Three Bridges Park wetland lowland plot where the relationship was negative.

The advection-diffusion-reaction model simulations implied that the variability of ARQ is driven primarily by biogeochemical process response to soil moisture rather than physical processes associated with moisture transport in the unsaturated zone. When the biogeochemical processes were assumed to vary with soil moisture, the simulated ARQ values decreased to values comparable to the field results. When only soil moisture was assumed to be variable, representing the physical response of advection and diffusion to soil moisture, the ARQ values remained similar to the control simulation results.

6.2 Future Work

Future work should include analyzing the variability in ARQ both temporally and spatially within the soil column (Hodges et al., 2019; Vargas et al., 2010). Deploying sensors at multiple depths within the GSI soils may provide more information on CO_2 and O_2 transport. Sensors at multiple depths may explain if CO_2 dissolution is occurring as well as abiotic contributions of CO_2.

Studies on nutrients, carbon sources, and metal concentrations in the influent, effluent, and soil could also improve the identification of biogeochemical processes. Nutrient speciation monitoring can assist in understanding the biogeochemical processes in the GSI soils. Metal concentration could improve the explanation of low ARQ readings due to reduced metal oxidation (Sánchez-Cañete et al., 2018). Carbon sources have also been reported to influence ARQ (Hicks Pries et al., 2019). Carbon sources can further explain the ability of microbes and roots to take up nutrients and focus on nutrient use efficiency rather than carbon use efficiency (Manzoni et al., 2012; Yuan et al., 2019).

Better identification of what biogeochemical processes are occurring in these soils should be ventured next. This research has found that biogeochemical processes were occurring in these soils and were highly variable in response to hydro-climatic changes. Accurately identifying what these processes are can improve recommendations for the GSI design to remove nutrients. Including measurements of other gases like N_2O, N_2, and CH_4 at a high frequency may assist in the identification of anaerobic metabolism in soils. Denitrification is a process that could better link ARQ to nutrient uptake and use. If able to monitor the denitrification rates in GSI, this may dramatically improve how to test GSI design and soil conditions that denitrifiers favor. Also, monitoring CH_4 can assist in identifying whether anaerobic activity is occurring as well as comparing methane oxidation in the field to the stoichiometric CO_2:O_2 ratio. The analysis from this study suggested the biological activity was either not accurately represented by the stoichiometric CO_2:O_2 ratios or that multiple processes were co-occurring with biological respiration. By monitoring other gases, one could better interpret if other processes are occurring at the same time as biological respiration. Also, conducting a rRNA test on soil samples to determine what microbial communities are present in the GSI soils would be helpful for future work. Knowing the active microbial communities would then draw a clearer analysis of the ARQ readings from the field.

7. BIBLIOGRAPHY

Amundson, R., Richter, D. D., Humphreys, G. S., Jobbágy, E. G., & Gaillardet, J. (2007). Coupling between biota and earth materials in the critical zone. *Elements*, *3*(5), 327–332. https://doi.org/10.2113/gselements.3.5.327

Angert, A., & Sherer, Y. (2011). Determining the relationship between tree-stem respiration and CO2 efflux by δO2/Ar measurements. *Rapid Communications in Mass Spectrometry*, *25*(12), 1752–1756. https://doi.org/10.1002/rcm.5042

Angert, A., Yakir, D., Rodeghiero, M., Preisler, Y., Davidson, E. A., & Weiner, T. (2015). Using O2 to study the relationships between soil CO2 efflux and soil respiration. *Biogeosciences*, *12*(7), 2089–2099. https://doi.org/10.5194/bg-12-2089-2015

Avellandeda, P. M., Jefferson, A. J., Grieser, J. M., & Bush, S. A. (2017). Simulation of the cumulative hydrological response to green infrastructure. *WATER RESOURCES RESEARCH*, *53*, 3087–3101. https://doi.org/10.1002/ 2016WR019836

Bannerman, R., & Considine, E. (2003). Rain Gardens: A How To For Home-owners. *DNR & UW Extension*, 1–32.

Berg, M., Meehan, M., Franzen, D., Scherer, T., Wiederholt, R., & Johnson, B. (2018). *Phosphorus Behavior In the Environment*. *NDSU Extension* (Vol. 1298).

Bettez, N. D., & Groffman, P. M. (2012). Denitrification potential in stormwater control structures and natural riparian zones in an urban landscape. *Environmental Science and Technology*, *46*(20), 10909–10917. https://doi.org/10.1021/es301409z

Blecken, G. T., Zinger, Y., Muthanna, T. M., Deletic, A., Fletcher, T. D., & Viklander, M. (2007). The influence of temperature on nutrient treatment efficiency in stormwater biofilter systems. *Water Science and Technology*, *56*(10), 83–91. https://doi.org/10.2166/wst.2007.749

Bratieres, K., Fletcher, T. D., Deletic, A., & Zinger, Y. (2008). Nutrient and sediment removal by stormwater biofilters: A large-scale design optimisation study. *Water Research*, *42*(14), 3930–3940. https://doi.org/10.1016/j.watres.2008.06.009

Buffam, I., & Mitchell, M. E. (2015). Nutrient Cycling in Green Roof Ecosystems. In *Green Roof Ecosystems* (pp. 107–137). Springer International Publishing Switzerland. https://doi.org/10.1007/978-3-319-14983-7_5

Burgin, A. J., Yang, W. H., Hamilton, S. K., & Silver, W. L. (2011). Beyond carbon and nitrogen: How the microbial energy economy couples elemental cycles in diverse ecosystems. *Frontiers in Ecology and the Environment*, *9*(1), 44–52. https://doi.org/10.1890/090227

Calmels, D., Gaillardet, J., & François, L. (2014). Sensitivity of carbonate weathering to soil CO 2 production by biological activity along a temperate climate transect.

Chemical Geology, *390*(November), 74–86. https://doi.org/10.1016/j.chemgeo.2014.10.010

Carey, R. O., Hochmuth, G. J., Martinez, C. J., Boyer, T. H., Dukes, M. D., Toor, G. S., & Cisar, J. L. (2013). Evaluating nutrient impacts in urban watersheds: Challenges and research opportunities. *Environmental Pollution*, *173*, 138–149. https://doi.org/10.1016/j.envpol.2012.10.004

Celia, M. A., & Bouloutas, E. T. (1990). A General Mass-Conservation Numerical Solution for the Unsaturated Flow Equation. *Water Resources Research*, *26*(7), 1483–1496.

Chahal, M. K., Shi, Z., & Flury, M. (2016). Nutrient leaching and copper speciation in compost-amended bioretention systems. *Science of the Total Environment*, *556*, 302–309. https://doi.org/10.1016/j.scitotenv.2016.02.125

Collins, K. A., Lawrence, T. J., Stander, E. K., Jontos, R. J., Kaushal, S. S., Newcomer, T. A., et al. (2010). Opportunities and challenges for managing nitrogen in urban stormwater: A review and synthesis. *Ecological Engineering*. https://doi.org/10.1016/j.ecoleng.2010.03.015

Daly, E., Deletic, A., Hatt, B. E., & Fletcher, T. D. (2012). Modelling of stormwater biofilters under random hydrologic variability: a case study of a car park at Monash University, Victoria (Australia). *Hydrological Processes*, *26*(22), 3416–3424. https://doi.org/10.1002/hyp.8397

Dancer, W. S., Peterson, L. A., & Chesters, G. (1973). Ammonification and Nitrification of N as Influenced by Soil pH and Previous N Treatments. *Soil Science Society of America*, *37*(1), 67–69.

Daniel J. Conley, Hans W. Paerl, Robert W. Howarth, Donald F. Boesch, Sybil P. Seitzinger, Karl E. Havens, et al. (2009). Controlling Eutrophication: Nitrogen and Phosphorus. *Science*, *323*, 1014–1015. Retrieved from http://www.sciencemag.org/content/323/5917/1014.summary

Davidson, E. A., Savage, K., Verchot, L. V., & Navarro, R. (2002). Minimizing artifacts and biases in chamber-based measurements of soil respiration. *Agricultural and Forest Meteorology*, *113*(1–4), 21–37. https://doi.org/10.1016/S0168-1923(02)00100-4

Davis, A. P. (2005). Green engineering principles promote low-impact development. *Environmental Science and Technology*. https://doi.org/10.1021/es053327e

Davis, A. P. (2007). Field Performance of Bioretention: Water Quality. *ENVIRONMENTAL ENGINEERING SCIENCE*, *24*(8). https://doi.org/10.1089/ees.2006.0190

Davis, A. P., Shokouhian, M., Sharma, H., & Minami, C. (2006). Water Quality Improvement through Bioretention Media: Nitrogen and Phosphorus Removal. *Water Environment Research*, *78*(3), 284–293. https://doi.org/10.2175/106143005x94376

Davis, A. P., Traver, R. G., & Hunt, W. F. (2010). Improving Urban Stormwater Quality: Applying Fundamental Principles. *Journal of Contemporary Water Research & Education*, (146), 3–10. https://doi.org/10.1002/ar.1090960209

Deangelis, K. M., Silver, W. L., Thompson, A. W., & Firestone, M. K. (2012). Microbial communities acclimate to recurring changes in soil redox potential statuse mi_2286 3137..3149. *Environmental Microbiology*, *12*(12), 3137–3149. https://doi.org/10.1111/j.1462-2920.2010.02286.x

Deeb, M., Groffman, P. M., Joyner, J. L., Lozefski, G., Paltseva, A., Lin, B., et al. (2018). Soil and microbial properties of green infrastructure stormwater management systems. *Ecological Engineering*, *125*(November), 68–75. https://doi.org/10.1016/j.ecoleng.2018.10.017

Dietz, M. E., & Clausen, J. C. (2005). A FIELD EVALUATION OF RAIN GARDEN FLOW AND POLLUTANT TREATMENT. *Water, Air, and Soil Pollution*, *167*(1–4), 123–138. https://doi.org/https://doi.org/10.1007/s11270-005-8266-8

DNR, W. (2014). *Final Guidance: Technical Standard 1004 - Bioretention for Infiltration*. Retrieved from https://dnr.wi.gov/news/input/documents/guidance/BioretentionGuidanceFinal.pdf

Earth System Research Laboratory. (2019). Trends in Atmospheric Carbon Dioxide. Retrieved from https://www.esrl.noaa.gov/gmd/ccgg/trends/

Elberling, B., Askaer, L., Jørgensen, C. J., Joensen, H. P., Kühl, M., Glud, R. N., & Lauritsen, F. R. (2011). Linking soil O2, CO2, and CH4 concentrations in a wetland soil: Implications for CO2 and CH 4 fluxes. *Environmental Science and Technology*, *45*(8), 3393–3399. https://doi.org/10.1021/es103540k

Fang, C., & Moncrieff, J. B. (1998). An open-top chamber for measuring soil respiration and the influence of pressure difference on CO2 efflux measurement. *Functional Ecology*, *12*(2), 319–325. https://doi.org/10.1046/j.1365-2435.1998.00189.x

Fenchel, T., King, G. M., Blackburn, T. H., Fenchel, T., King, G. M., & Blackburn, T. H. (2012). *Bacterial Biogeochemistry: the Ecophysiology of Mineral Cycling*. *Bacterial Biogeochemistry* (3rd ed.). Academic Press. https://doi.org/10.1016/B978-0-12-415836-8.00003-7

Ferraz de Almeida, R., de Bortoli Teixeira, D., Montanari, R., Bolonhezi, A. C., Teixeira, E. B., Moitinho, M. R., et al. (2018). Ratio of CO2 and O2 as index for categorising soil biological activity in sugarcane areas under contrasting straw management regimes. *Soil Research*, *56*(4), 373. https://doi.org/10.1071/sr16344

Field, R., Muthukrishnan, S., Madge, B., Selvakumar, A., & Sullivan, D. (2004). *The Use of Best Management Practices (BMPs) in Urban Watersheds*. Cincinnati. Retrieved from https://nepis.epa.gov/Exe/ZyNET.exe/P100O0RJ.txt?ZyActionD=ZyDocument&Client=EPA&Index=2000 Thru 2005&Docs=&Query=&Time=&EndTime=&SearchMethod=1&TocRestrict=n&Toc=&TocEntry=&QField=&QFieldYear=&QFieldMonth=&QFieldDay=&UseQField

=&IntQFieldOp=0&ExtQFieldOp=

Fierer, N., & Jackson, R. B. (2006). The diversity and biogeography of soil bacterial communities. *Proceedings of the National Academy of Sciences of the United States of America*, *103*(3), 626–631. https://doi.org/10.1073/pnas.0507535103

Gao, G., Wang, J., Guo, W., & Pei, Y. S. (2010). Nitrogen removal from three-stage oxidation-reduction system by simulation of the riparian environment. *Procedia Environmental Sciences*, *2*(5), 1997–2004. https://doi.org/10.1016/j.proenv.2010.10.215

Groffman, P. M., & Crawford, M. K. (2003). Denitrification potential in urban riparian zones. *Journal of Environmental Quality*, *32*(3), 1144–1149. https://doi.org/10.2134/jeq2003.1144

Groffman, P. M., Law, N. L., Belt, K. T., Band, L. E., & Fisher, G. T. (2004). Nitrogen fluxes and retention in urban watershed ecosystems. *Ecosystems*, *7*(4), 393–403. https://doi.org/10.1007/s10021-003-0039-x

Hall, S. J., Mcdowell, W. H., & Silver, W. L. (2013). When Wet Gets Wetter: Decoupling of Moisture, Redox Biogeochemistry, and Greenhouse Gas Fluxes in a Humid Tropical Forest Soil. *Ecosystems*, *16*, 576–589. https://doi.org/10.1007/s10021-012-9631-2

Hatt, B.E., Fletcher, T. D., & Deletic, A. (2007). Hydraulic and pollutant removal performance of stormwater filters under variable wetting and drying regimes. *Water Science and Technology*, *56*(12), 11–19. https://doi.org/10.2166/wst.2007.751

Hatt, Belinda E., Fletcher, T. D., & Deletic, A. (2009). Hydrologic and pollutant removal performance of stormwater biofiltration systems at the field scale. *Journal of Hydrology*, *365*(3–4), 310–321. https://doi.org/10.1016/j.jhydrol.2008.12.001

Hicks Pries, C. E., Castanha, C., Porras, R., Phillips, C., & Torn, M. S. (2018). Response to Comment on "The whole-soil carbon flux in response to warming." *Science (New York, N.Y.)*, *359*(6378), 1420–1423. https://doi.org/10.1126/science.aao0457

Hicks Pries, C. E., Angert, A., Castanha, C., Hilman, B., & Torn, M. S. (2019). Using Respiration Quotients to Track Changing Sources of Soil Respiration Seasonally and with Experimental Warming. *Biogeosciences Discussions*, (June), 1–20. https://doi.org/10.5194/bg-2019-232

Hobbie, S. E., Finlay, J. C., Benjamin, D., Nidzgorski, D. A., Millet, D. B., Lawrence, A., et al. (2017). Correction: Contrasting nitrogen and phosphorus budgets in urban watersheds and implications for managing urban water pollution (Proceedings of the National Academy of Sciences of the United States of America (2017) 114 (4177-4182) DOI: 10.1073/pnas.16185. *Proceedings of the National Academy of Sciences of the United States of America*, *114*(20), E4116. https://doi.org/10.1073/pnas.1706049114

Hodges, C., Kim, H., & Brantley, S. L. (2019). Soil CO2 and O2 Concentrations Illuminate the Relative Importance of Weathering and Respiration to Seasonal Soil

Gas Fluctuations. *Soil Science Society of America Journal*, *83*(4), 1167–1180.

Hunt, W. F., Jarrett, A. R., Smith, J. T., & Sharkey, L. J. (2006). Evaluating Bioretention Hydrology and Nutrient Removal at Three Field Sites in North Carolina. *Journal of Irrigation and Drainage Engineering*, *132*(6), 600–608. https://doi.org/10.1061/ASCE0733-94372006132:6600

Hurley, S., Shrestha, P., & Cording, A. (2017). Nutrient Leaching from Compost: Implications for Bioretention and Other Green Stormwater Infrastructure. *Journal of Sustainable Water in the Built Environment*, *3*(3), 04017006. https://doi.org/10.1061/jswbay.0000821

Iiyama, I., & Hasegawa, S. (2009). In situ CO2 profiles with complementary monitoring of O 2 in a drained peat layer. *Soil Science and Plant Nutrition*, *55*(1), 26–34. https://doi.org/10.1111/j.1747-0765.2008.00331.x

Jarden, K. M., Jefferson, A. J., & Grieser, J. M. (2016). Assessing the effects of catchment-scale urban green infrastructure retrofits on hydrograph characteristics. *Hydrological Processes*, *30*(10), 1536–1550. https://doi.org/10.1002/hyp.10736

Jiao, F., Shi, X. R., Han, F. P., & Yuan, Z. Y. (2016). Increasing aridity, temperature and soil pH induce soil C-N-P imbalance in grasslands. *Scientific Reports*, *6*(January), 1–9. https://doi.org/10.1038/srep19601

Kaye, J. P., Groffman, P. M., Grimm, N. B., Baker, L. A., & Pouyat, R. V. (2006). A distinct urban biogeochemistry? *Trends in Ecology and Evolution*, *21*(4), 192–199. https://doi.org/10.1016/j.tree.2005.12.006

Kessler, T. J., & Harvey, C. F. (2001). The global flux of carbon dioxide into groundwater. *Geophysical Research Letters*, *28*(2), 279–282.

Kim, H., Seagren, E. A., & Davis, A. P. (2003). Engineered Bioretention for Removal of Nitrate from Stormwater Runoff. *Water Environment Research*, *75*(4), 355–367. Retrieved from http://www.jstor.org/stable/25045707

Knobeloch, L., Salna, B., Hogan, A., Postle, J., & Anderson, H. (2000). Blue babies and nitrate-contaminated well water. *Environmental Health Perspectives*, *108*(7), 675–678. https://doi.org/10.1289/ehp.00108675

Lasaga, A. C. (1984). Chemical Kinetics of Water-Rock Interactions. *Journal of Geophysical Research*, *89*(4), 4009–4025.

Law, B. E., Ryan, M. G., & Anthoni, P. M. (1999). Seasonal and annual respiration of a ponderosa pine. *Global Change Biology*, *5*, 169–182.

Li, L., & Davis, A. P. (2014). Urban stormwater runoff nitrogen composition and fate in bioretention systems. *Environmental Science and Technology*, *48*(6), 3403–3410. https://doi.org/10.1021/es4055302

Li, W., Jin, C., Guan, D., Wang, Q., Wang, A., Yuan, F., & Wu, J. (2015). The effects of simulated nitrogen deposition on plant root traits: A meta-analysis. *Soil Biology and Biochemistry*, *82*(October), 112–118. https://doi.org/10.1016/j.soilbio.2015.01.001

Lin, T., Gibson, V., Cui, S., Yu, C. P., Chen, S., Ye, Z., & Zhu, Y. G. (2014). Managing urban nutrient biogeochemistry for sustainable urbanization. *Environmental Pollution*, *192*, 244–250. https://doi.org/10.1016/j.envpol.2014.03.038

Liptzin, D., Silver, W. L., & Detto, M. (2011). Temporal Dynamics in Soil Oxygen and Greenhouse Gases in Two Humid Tropical Forests. *Ecosystems*, *14*, 171–182. https://doi.org/10.1007/s10021-010-9402-x

Liu, J., & Davis, A. P. (2014). Phosphorus speciation and treatment using enhanced phosphorus removal bioretention. *Environmental Science and Technology*, *48*(1), 607–614. https://doi.org/10.1021/es404022b

Liu, Y., Lawrence, C. R., Winnick, M. J., Hsu, H. T., Maher, K., & Druhan, J. L. (2019). Modeling Transient Soil Moisture Limitations on Microbial Carbon Respiration. *Journal of Geophysical Research: Biogeosciences*, *124*(7), 2222–2247. https://doi.org/10.1029/2018JG004628

Livingston, B., Frost, J., Sventek, J., Chapman, J., Clay, R., Colvin, S., et al. (2019). Minnesota Stormwater Manual. Retrieved from https://stormwater.pca.state.mn.us/index.php?title=Design_criteria_for_bioretention

Lloyd, J., & Taylor, J. A. (1994). On the Temperature Dependence of Soil Respiration. *Functional Ecology*, *8*(3), 315. https://doi.org/10.2307/2389824

Lopez-Ponnada, E. V., Lynn, T. J., Peterson, M., Ergas, S. J., & Mihelcic, J. R. (2017). Application of denitrifying wood chip bioreactors for management of residential non-point sources of nitrogen. *Journal of Biological Engineering*, *11*(1), 16. https://doi.org/10.1186/s13036-017-0057-4

Ma, J., Wang, Z. Y., Stevenson, B. A., Zheng, X. J., & Li, Y. (2013). An inorganic CO2 diffusion and dissolution process explains negative CO2 fluxes in saline/alkaline soils. *Scientific Reports*, *3*, 1–7. https://doi.org/10.1038/srep02025

Maher, K., & Chamberlain, C. P. (2014). Hydrologic Regulation of Chemical Weathering and the Geologic Carbon Cycle. *Science*, *343*(March), 1502–1504. https://doi.org/10.1126/science.1250770

Manzoni, S., Taylor, P., Richter, A., Porporato, A., & Ågren, G. I. (2012). Environmental and stoichiometric controls on microbial carbon-use efficiency in soils. *New Phytologist*, *196*(1), 79–91. https://doi.org/10.1111/j.1469-8137.2012.04225.x

Marschner, H. (2012). *Marschner's Mineral Nutrition of Higher Plants*. (P. MARSCHNER, Ed.) (third). San Diago: Academic Press. Retrieved from https://books.google.com/books?hl=en&lr=&id=yqKV3USG41cC&oi=fnd&pg=PP1&dq=Marchner++Mineral+Nutrition+of+Higher+Plants+1995&ots=Vb9LS8CZCd&sig=J7h-_2lMkuzzr55UKzYly1XC91I#v=onepage&q&f=false

McPhillips, L., & Walter, M. T. (2015). Hydrologic conditions drive denitrification and greenhouse gas emissions in stormwater detention basins. *Ecological Engineering*, *85*, 67–75. https://doi.org/10.1016/j.ecoleng.2015.10.018

McPhillips, L., Groffman, P. M., Schneider, R. L., & Walter, M. T. (2016). Nutrient

Cycling in Grassed Roadside Ditches and Lawns in a Suburban Watershed. *Journal of Environmental Quality*, *45*(6), 1901–1909. https://doi.org/10.2134/jeq2016.05.0178

Moore, T. R., & Dalva, M. (1993). The influence of temperature and water table position on carbon dioxide and methane emissions from laboratory columns of peatland soils. *Journal of Soil Science*, *44*(4), 651–664. https://doi.org/10.1111/j.1365-2389.1993.tb02330.x

Moyano, F. E., Vasilyeva, N., Bouckaert, L., Cook, F., Craine, J., Curiel Yuste, J., et al. (2012). The moisture response of soil heterotrophic respiration: Interaction with soil properties. *Biogeosciences*, *9*(3), 1173–1182. https://doi.org/10.5194/bg-9-1173-2012

Moyano, F. E., Manzoni, S., & Chenu, C. (2013). Responses of soil heterotrophic respiration to moisture availability: An exploration of processes and models. *Soil Biology and Biochemistry*, *59*, 72–85. https://doi.org/10.1016/j.soilbio.2013.01.002

NAE. (2012). The Grand Challenges for Engineering in 21st century. *National Academy of Sciences*.

National Pollutant Removal Performance Database. (2007). Retrieved from http://www.cwp.org

Newcomer Johnson, T. A., Kaushal, S. S., Mayer, P. M., & Grese, M. M. (2014). Effects of stormwater management and stream restoration on watershed nitrogen retention. *Biogeochemistry*, *121*(1), 81–106. https://doi.org/10.1007/s10533-014-9999-5

Norton, R. A., Harrison, J. A., Kent Keller, C., & Moffett, K. B. (2017). Effects of storm size and frequency on nitrogen retention, denitrification, and N2O production in bioretention swale mesocosms. *Biogeochemistry*, *134*(3), 353–370. https://doi.org/10.1007/s10533-017-0365-2

Nylen, N. G., & Kiparsky, M. (2015). *Accelerating Cost-Effective Green Stormwater Infrastructure : Learning from local implementation*. Berkeley, California.

Okochi, N. C., & McMartin, D. W. (2011). Laboratory investigations of stormwater remediation via slag: Effects of metals on phosphorus removal. *Journal of Hazardous Materials*, *187*(1–3), 250–257. https://doi.org/10.1016/j.jhazmat.2011.01.015

Olshansky, Y., Knowles, J. F., Barron-gafford, G. A., Rasmussen, C., & Chorover, J. (2019). Soil fluid biogeochemical response to climatic events. *JGR Biogeosciences*, 1–23. https://doi.org/10.1029/2019JG005216

Orchard, V. A., & Cook, F. J. (1983). Relationship between soil respiration and soil moisture. *Soil Biology and Biochemistry*, *15*(4), 447–453. https://doi.org/10.1016/0038-0717(83)90010-X

Pataki, D. E., Carreiro, M. M., Cherrier, J., Grulke, N. E., Jennings, V., Pincetl, S., et al. (2011). Coupling biogeochemical cycles in urban environments: Ecosystem services, green solutions, and misconceptions. *Frontiers in Ecology and the*

Environment, *9*(1), 27–36. https://doi.org/10.1890/090220

Patrick, W. H., & Jugsujinda, A. (1992). Sequential Reduction and Oxidation of Inorganic Nitrogen, Manganese, and Iron in Flooded Soil. *Soil Science Society of America*, *56*, 1071–1073. https://doi.org/10.2136/sssaj1992.03615995005600040011x

Paul, M. J., & Meyer, J. L. (2001). Streams in the Urban Landscape. *Annual Review of Ecology and Systematics*, *32*, 333–365. https://doi.org/0066-4162/01/1215-0333

Payne, E. G. I., Pham, T., Cook, P. L. M., Fletcher, T. D., Hatt, B. E., & Deletic, A. (2014). Biofilter design for effective nitrogen removal from stormwater-influence of plant species, inflow hydrology and use of a saturated zone. *Water Science & Technology*, 1312–1319. https://doi.org/10.2166/wst.2014.013

Pett-Ridge, J., Silver, W. L., & Firestone, M. K. (2006). Redox fluctuations frame microbial community impacts on N-cycling rates in a humid tropical forest soil. *Biogeochemistry*, *81*, 95–110. https://doi.org/10.1007/s10533-006-9032-8

Pouyat, R. V, Yesilonis, I. D., Groffman, P. M., Szlavecz, K., & Schwarz, K. (2010). Chemical, Physical, and Biological Characteristics of Urban Soils. *Agronomy Monograph 55. Urban Ecosystem Ecology*, *0129*, 119–152. https://doi.org/10.2134/agronmonogr55.c7

Raich, J. W., & Schlesinger, W. H. (1992). The global carbon dioxide flux in soil respiration and its relationship to vegetation and climate. *Tellus B*, *44*(2), 81–99. https://doi.org/10.1034/j.1600-0889.1992.t01-1-00001.x

Reddy, K. R., & Patrick, W. H. (1975). Effect of alternate aerobic and anaerobic conditions on redox potential, organic matter decomposition and nitrogen loss in a flooded soil. *Soil Biology and Biochemistry*, *7*(2), 87–94. https://doi.org/10.1016/0038-0717(75)90004-8

Risk, D., Kellman, L., & Beltrami, H. (2002). Carbon dioxide in soil profiles: Production and temperature dependence. *Geophysical Research Letters*, *29*(6), 11-1-11–4. https://doi.org/10.1029/2001GL014002

Riveros-Iregui, D. A., Emanuel, R. E., Muth, D. J., McGlynn, B. L., Epstein, H. E., Welsch, D. L., et al. (2007). Diurnal hysteresis between soil CO 2 and soil temperature is controlled by soil water content. *Geophysical Research Letters*, *34*(17), 1–5. https://doi.org/10.1029/2007GL030938

Riveros-Iregui, D. A., McGlynn, B. L., Marshall, L. A., Welsch, D. L., Emanuel, R. E., & Epstein, H. E. (2011). A watershed-scale assessment of a process soil CO2 production and efflux model. *Water Resources Research*, *47*(5), 1–12. https://doi.org/10.1029/2010WR009941

Rode, M., Wade, A. J., Cohen, M. J., Hensley, R. T., Bowes, M. J., Kirchner, J. W., et al. (2016). Sensors in the Stream: The High-Frequency Wave of the Present. *Environmental Science and Technology*, *50*(19), 10297–10307. https://doi.org/10.1021/acs.est.6b02155

Romanak, K. D., Bennett, P. C., Yang, C., & Hovorka, S. D. (2012). Process-based approach to CO2 leakage detection by vadose zone gas monitoring at geologic CO2 storage sites. *Geophysical Research Letters*, *39*(15), 1–7. https://doi.org/10.1029/2012GL052426

Rubol, S., Silver, W. L., & Bellin, A. (2012). Hydrologic control on redox and nitrogen dynamics in a peatland soil. *Science of The Total Environment*, *432*, 37–46. https://doi.org/10.1016/j.scitotenv.2012.05.073

Sahrawat, K. L. (1982). Nitrification in some tropical soils. *Plant and Soil*, *65*(2), 281–286. https://doi.org/10.1007/BF02374659

Salvucci, G. D., & Entekhabi, D. (1995). Ponded infiltration into soils bounded by a water table. *WATER RESOURCES RESEARCH*, *31*(11), 2751–2759. Retrieved from https://agupubs.onlinelibrary.wiley.com/doi/pdf/10.1029/95WR01954

Sánchez-Cañete, E. P., Barron-Gafford, G. A., & Chorover, J. (2018). A considerable fraction of soil-respired CO2 is not emitted directly to the atmosphere. *Scientific Reports*, *8*(1), 2–11. https://doi.org/10.1038/s41598-018-29803-x

Schlesinger, W. H., & Bernhardt, E. S. (2013). *Biogeochemistry: An Analysis of Global Change* (3rd ed.). Academic Press. Retrieved from https://books.google.com/books?id=533UOWBU3_AC&printsec=frontcover&source=gbs_ge_summary_r&cad=0#v=onepage&q&f=false

Schlüter, S., Zawallich, J., Vogel, H.-J., & Dörsch, P. (2019). Physical constraints for respiration in microbial hotspots in soil and their importance for denitrification. *Biogeosciences Discussions*, *16*(18), 1–31. https://doi.org/10.5194/bg-2019-2

Sierra, C. A., Malghani, S., & Loescher, H. W. (2017). Interactions among temperature, moisture, and oxygen concentrations in controlling decomposition rates in a boreal forest soil. *Biogeosciences*, *14*(3), 703–710. https://doi.org/10.5194/bg-14-703-2017

Silver, W. L., Scatena, F. N., Johnson, A. H., Siccama, T. G., & Sanchez, M. J. (1994). Nutrient availability in a montane wet tropical forest: Spatial patterns and methodological considerations. *Plant and Soil*, *164*(1), 129–145. https://doi.org/10.1007/BF00010118

Silver, W. L., Lugo, A. E., & Keller, M. (1999). Soil oxygen availability and biogeochemistry along rainfall and topographic gradients in upland wet tropical forest soils. *Biogeochemistry*, *44*(3), 301–328. https://doi.org/10.1023/A:1006034126698

Simunek, J., & Suarez, D. L. (1993). Modeling of Carbon Dioxide Transport and Production in Soil. *Water Resources Research*, *29*(2), 487–497.

Smith, D. R., King, K. W., & Williams, M. R. (2015). What is causing the harmful algal blooms in Lake Erie? *Journal of Soil and Water Conservation*, *70*(2), 27A-29A. https://doi.org/10.2489/jswc.70.2.27A

Smith, V. H., Tilman, G. D., & Nekola, J. C. (1999). Eutrophication: Impacts of excess nutrient inputs on freshwater, marine, and terrestrial ecosystems. *Environmental*

Pollution, *100*(1–3), 179–196. https://doi.org/10.1016/S0269-7491(99)00091-3

Soetaert, K., Hofmann, A. F., Middelburg, J. J., Meysman, F. J. R., & Greenwood, J. (2007). The effect of biogeochemical processes on pH. *Marine Chemistry*, *105*(1–2), 30–51. https://doi.org/10.1016/j.marchem.2006.12.012

Strauss, E. A., Mitchell, N. L., & Lamberti, G. A. (2002). Factors regulating nitrification in aquatic sediments: Effects of organic carbon, nitrogen availability, and pH. *Canadian Journal of Fisheries and Aquatic Sciences*, *59*(3), 554–563. https://doi.org/10.1139/f02-032

U.S. Environmental Protection Agency (EPA). (2010). *Green Infrastructure Case Study: Municipal Policies for Managing Stormwater with Green Infrastructure*. *EPA-841-F-10-004*.

United States Environmental Protection Agency (EPA). (2017). *National Water Quality Inventory: Report to Congress, EPA 841-R-16-011*. Retrieved from http://www.ncbi.nlm.nih.gov/pubmed/2347274

United States Environmental Protection Agency (EPA). (2019). Nutrient Pollution. Retrieved January 12, 2019, from https://www.epa.gov/nutrientpollution/issue

Vargas, R., Detto, M., Baldocchi, D. D., & Allen, M. F. (2010). Multiscale analysis of temporal variability of soil CO2 production as influenced by weather and vegetation. *Global Change Biology*, *16*(5), 1589–1605. https://doi.org/10.1111/j.1365-2486.2009.02111.x

Walsh, C. J., Roy, A. H., Feminella, J. W., Cottingham, P. D., Groffman, P. M., & Morgan, R. P. (2005). The urban stream syndrome: current knowledge and the search for a cure. *Journal of the North American Benthological Society*, *24*(3), 706–723. https://doi.org/10.1899/04-028.1

Wang, L., Lyons, J., Kanehl, P., & Bannerman, R. (2001). Impacts of Urbanization on Stream Habitat and Fish Across Multiple Spatial Scales. *Environmental Management*, *28*(2), 255–266. https://doi.org/10.1007/s002670010222

Wang, S., Lin, X., Yu, H., Wang, Z., Xia, H., An, J., & Fan, G. (2017). Nitrogen removal from urban stormwater runoff by stepped bioretention systems. *Ecological Engineering*, *106*(September), 340–348. https://doi.org/10.1016/j.ecoleng.2017.05.055

WDNR. (2018). Wisconsin's 2018 impaired waters list. Retrieved from https://dnr.wi.gov/topic/impairedwaters/2018IR_IWList.html

White, A. F., & Blum, A. (1995). Effects of climate on Chemical Weathering in Watersheds. *Geochimica et Cosmochimica Acta*, *59*(9), 1729–1747.

Xiang, S. R., Doyle, A., Holden, P. A., & Schimel, J. P. (2008). Drying and rewetting effects on C and N mineralization and microbial activity in surface and subsurface California grassland soils. *Soil Biology and Biochemistry*, *40*(9), 2281–2289. https://doi.org/10.1016/j.soilbio.2008.05.004

Yang, B., & Li, S. (2013). Green Infrastructure Design for Stormwater Runoff and Water Quality: Empirical Evidence from Large Watershed-Scale Community Developments. *Water*, *5*(4), 2038–2057. https://doi.org/10.3390/w5042038

Yuan, X., Niu, D., Gherardi, L. A., Liu, Y., Wang, Y., Elser, J. J., & Fu, H. (2019). Linkages of stoichiometric imbalances to soil microbial respiration with increasing nitrogen addition: Evidence from a long-term grassland experiment. *Soil Biology and Biochemistry*, *138*(August), 107580. https://doi.org/10.1016/j.soilbio.2019.107580

Zhang, Q., Katul, G. G., Oren, R., Daly, E., Manzoni, S., & Yang, D. (2015). The hysteresis response of soil CO 2 concentration and soil respiration to soil temperature. *Journal of Geophysical Research: Biogeosciences*, *120*(8), 1605–1618. https://doi.org/10.1002/2015JG003047

Zhang, Q., Phillips, R. P., Manzoni, S., Scott, R. L., Oishi, A. C., Finzi, A., et al. (2018). Changes in photosynthesis and soil moisture drive the seasonal soil respiration-temperature hysteresis relationship. *Agricultural and Forest Meteorology*, *259*(March), 184–195. https://doi.org/10.1016/j.agrformet.2018.05.005

Zhu, W.-X., Dillard, N. D., & Grimm, N. B. (2005). Urban nitrogen biogeochemistry: status and processes in green retention basins. *Biogeochemistry*, *71*(2), 177–196. https://doi.org/10.1007/s10533-005-0683-7